DESIGN AND IMPLEMENTATION OF CONVERTERS FOR ELECTRIC VEHICLE APPLICATIONS

A DISSERTATION

SUBMITTED IN PARTIAL FULFILLMENT OF THE RQUIREMENTS
FOR THE AWARD OF THE DEGREE
OF

MASTER OF TECHNOLOGY
IN
POWER ELECTRONICS AND SYSTEM

Submitted by:

Arya Singh
2K20/PES/05

Under the supervision of

Prof. Madhusudan Singh

DEPARTMENT OF ELECTRICAL ENGINEERING
DELHI TECHNOLOGICAL UNIVERSITY
(Formerly Delhi College of Engineering)
Bawana Road, Delhi-110042

June 2022

DEPARTMENT OF ELECTRICAL ENGINEERING

DELHI TECHNOLOGICAL UNIVERSITY
(Formerly Delhi College of Engineering)
Bawana Road, Delhi-110042

CERTIFICATE

I, **Arya Singh**, Roll No. 2K20/PES/05 student of **M. Tech. (Power Electronics and System)**, hereby declare that the dissertation titled **"DESIGN AND OF IMPLEMENTATION OF CONVERTERS FOR ELECTRIC VEHICLE APPLICATIONS"** under the supervision of Prof. Madhusudan Singh, Professor, Department of Electrical Engineering, Delhi Technological University in partial fulfillment of the requirement for the award of the degree of Master of Technology has not been submitted elsewhere for the award of any Other.

Place: Delhi **ARYA SINGH**

Date: 04.06.2022

Prof. MADHUSUDAN SINGH
Professor
Department of Electrical Engineering
Delhi Technological University

ACKNOWLEDGEMENT

I would like to express my sincere gratitude to Prof. Madhusudan Singh for his guidance and assistance in the thesis. The technical discussions with him were always been very insightful, and I will always be indebted to his for all the knowledge he shared with me. He always helped me in all the technical and non-technical issues during the preparation of this thesis. Without his consistent support, encouragement and valuable inputs, this project would not have become possible.

An assemblage of this nature could never have been attempted without reference to and inspiration from the works of others whose details are mentioned in reference section. I acknowledge my indebtedness to all of them.

I am thankful to all my classmates and the department research scholars for their co-operation and unfailing help during the project work.

I am grateful to all my friends who made my stay in Delhi, an unforgettable and rewarding experience.

Finally, I feel great reverence for all my family members and the Almighty, for their blessings and for being a constant source of encouragement.

ARYA SINGH

(2K20/PES/05) M.Tech (Power Electronics and System)
Delhi Technological University

ABSTRACT

Contemporary scientific and technical developments have enabled modern electronics to become more-compact and portable. The power electronics converters are playing crucial role in most of modern electronics gadgets that makes them appealing and practical. Different types of power electronic converters are utilized nowadays, like as DC-DC (chopper), AC-DC (rectifier), DC-AC (inverter), and AC-AC (Cyclo-Converter). Each of them has a particular use and is employed in some power electronics system. The present work demonstrates design and implementation of wireless power transfer (WPT) scheme using power electronics converter technology and also active clamp forward converter (ACFC).

Since power electronics are becoming more-small and portable by day, Wireless Power Transfer would be a interesting option for small and medium power charger for battery charging in electric vehicles (EVs). WPT is advantageous owing with two fundamental battery issues: short battery life and high initial cost. Several technologies have been proposed to increase the Wireless Transmission (WPT) capacity across a changeable range. Capacitive, inductive, & magnetic resonant coupling are some of the approaches for transferring wireless power, however these couplings do have limit on the power transfer values & range, indicating the inherent trade-off among distance & power transferred. This project is about using WPT for battery charging. There are three major sections in WPT: Conversion from DC-AC, wireless power transfer and AC- DC conversion. A single-switch resonant inverter will be used for DC-AC conversion to improve efficiency by eliminating component ON and OFF state losses. Magnetic Resonance Coupling (MRC) is used to transmit electricity wirelessly between two coils that function as sender and receiver. Eventually, a high frequency diode rectifier is employed to generate a DC output for charging the batteries. For the power amplifier, a class-E inverter is used, which works on a single-switch resonance phenomenon. The Class-E inverter does have the advantage of reducing switch stress. The converter operates at a switching frequency of 100 KHz & an efficiency of roughly 85.74 percent due to its single-switch design. High frequency operation reduces the size of the circuit components such as inductor and capacitor. MRC was used for WPT because it is more efficient for power transfer range over a variable distance in comparison to capacitive

and inductive resonant coupling. To acquire the most bandwidth for power transmission, an impedance matching approach is utilised. The DC output was obtained using a full-bridge rectifier circuit, which is used to charge a battery.

Active Clamp Forward Converter is a DC-DC converter with isolation which may be utilised for a wide variety of power of 50W to 500W i.e., for low-power applications, the ACFC is a common choice for single and/or multiple output power-supply. Active Clamp Forward Converter is used to harness power from battery of electric vehicles and transmit it to power up various other parts of electric vehicles. Active clamp forward converters are smaller and more efficient than passive clamp forward converters. In forward converter transformer's are utilised to accomplish circuit isolation and energy transformation from primary side to secondary side, as well as to reset the transformer's magnetising current using the active clamp approach. While there are a variety of approaches for accomplishing transformer reset, the active clamp approach is both simple and effective. ZVS (zero voltage switching), decreased switch voltage stress, wider duty cycle range, and reduced EMI (electro-magnetic interference) are just a few of the benefits of active switching. The active clamp approach uses a normal pulse width modulation (PWM) system to transmit power and the switch is switched on at zero-voltage-switching (ZVS) utilising transformers leakage-inductance (LL) and parasitic-capacitance and/or switch-output capacitance (CDS).

In this project efforts have been made to design a ACFC DC to DC converters for EV applications. The converter topology is simulated in MATLAB/Simulink and it's conversion capacity is demonstrated through relevant waveform and figure.

CONTENTS

LIST OF TABLES

LIST OF FIGURES

LEGENDS

Q_L	Quality Factor
W_S	Switching Frequency(ras/sec)
F_S	Switching Frequency(Hz)
K_C	Coupling Cofficient
1^0	Primary
2^0	Secondary
I/P	Input
O/P	Output
S/W	Switch
I_0	Output Current
V_0	Output Voltage
I_M	Peak Amplitude of Output Current
ϕ	Phase Difference
D	Duty Cycle
D_{min}	Minimum Duty Cycle
D_{min}	Minimum Duty Cycle
D_{max}	Maximum Duty Cycle
T	Time Period
V_P	Voltage at Transmitting Coil
I_P	Current at Transmitting Coil
V_S	Voltage at Receiving Coil
I_S	Current at Receiving Coil

L_P	Inductance of Transmitting Coil
C_P	Capacitance of Transmitting Coil
L_S	Inductance of Receiving Coil
C_S	Capacitance of Receiving Coil
L_L	Leakage Inductance
L_M	Magnetising Inductance
M	Mutual Inductance
C_{DS}	Mosfet Drain-Source Capacitance
I_{prms}	Transmitting Coil RMS Current
I_{srms}	Receiving Coil RMS Current
F_o	Resonant Frequency
S_M	Main Switch
S_{CL}	Clamp Switch
K_P	Proportional Gain
K_i	Integral Gain
η	Efficiency
N_P	Primary Number of Turns
N_S	Secondary Number of Turns
P_0	Output Power

ABBREVIATION AND ACRONYMS

WPT	Wireless Power Transfer
ZVS	Zero Voltage Switching
ZDS	Zero Derivative Switching
MRC	Magnetic Resonant Coupling
FWR	Full Bridge Diode Rectifier
ACFC	Active clamp forward converter
PWM	Pulse width modulation
ACFC	Active Clamp Forward Converter

CHAPTER 1

INTRODUCTION

1.1 INTRODUCTION

The processing & control of electric power flow is the focus of power electronic technology, which aims to produce voltage that are better suited to the demands of end users. A power electronic converter regulates and converts electric power using Semiconductor switches, Diodes, power-MOSFET, IGBT and some other power electronic components. The basic purpose of the converter is to create conditioned power for a particular application.

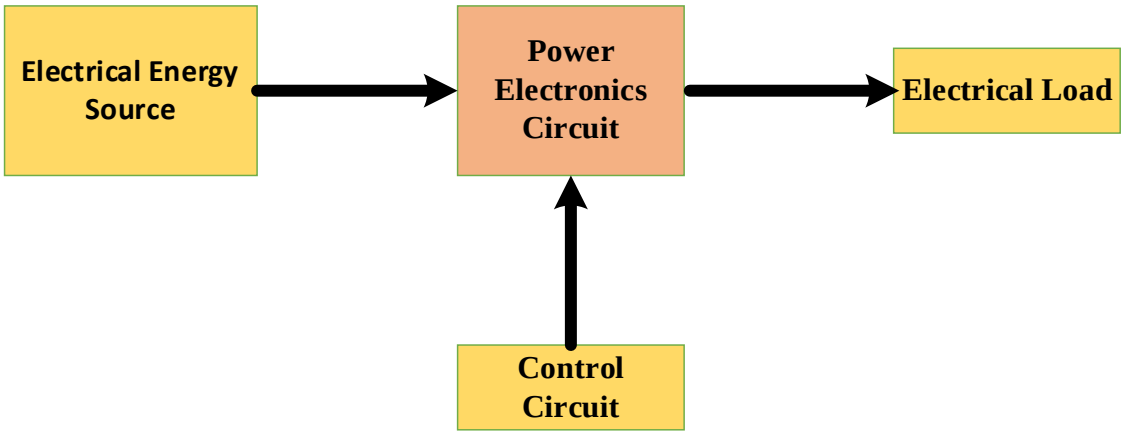

Fig. 1.1 Block Diagram of Power Electronics Converters.

In Fig.1.1, a block schematic of the power electronic converters is shown. This system consists of an electrical-power sources, a power semiconductor circuit, a control system, and an electrical load. This converter transforms one type of electrical energy into another. Both the power and control parts of a power electronic circuit are included. Power electronic switch (SCR, TRIAC, IGBT, MOSFET), transformer, electronic ballast, capacitors, fuses, and occasionally resistors make up the power portion, and it is a device that transfers energy from a source to a load. The control circuit block regulates the switching component of a converter's power section. This block is made up of an analogue or digital low-power electronic circuit. Power conversion is one of the most

basic functionalities of power converters. This converter is just a single energy conversion stage which can handle all AC / DC power conversion functions.

The following categories of power electronic converters had been created depending on the functions they perform.

- **Rectifier (AC-DC):** This transform alternating current_(AC) into pulsating Current_(DC).
- **Inverter (DC-AC):** This transforms DC to AC at the required Frequency & voltage.
- **Chopper (DC-DC):** It converts constant DC into variable DC and variable DC into constant DC.
- **Cyclo-converter (AC-AC):** This transforms AC from a line AC source to a specified frequency and/or voltage magnitude.

These types of power power converters are used in a variety of applications, including electric machine control, power storage, lighting drives, reactive and active filters, power generation and distribution, green power conversions, flexible AC transmissions, and embedded technology.

Power electronics converters were employed for electric vehicle applications. In this thesis design of wireless power transmission, used for charging electric vehicle batteries, and DC-DC converters using Active Clamped Forward Converter are described and simulation studies are presented for EV applications.

Without any electrical connections, energy can be sent from a sender to a receiver using WPT. WPT may technically be used to power any gadget. WPT is utilized in a variety of applications. Portable electronics and domestic gadgets are the most well-known WPT applications (e.g., smartphones, electric toothbrushes, wearables, smart watches). WPT is critical for biomedical implants including pacemakers, neurostimulators, and spinal cord stimulators [1].

Now a days technology is growing very rapidly. Engineers and scientists are pulling to technology at a new level. Before the 21st century most of the electrical and electronics devices and gadget were so bulky and wired. Normally, electric equipment is powered by an electrical cable that transmits electricity. However, the cable might be problematic at times since the equipment cannot travel from one location to another while being powered or charged. Battery as a power supply substitute is utilized for the mobility for electric equipment; nevertheless, various constraints of the battery, like as size, mass,

capacity, charging inconveniency, inability to give power for long periods of time, and so on, have not been adequately addressed. [2]-[5].

Device portability should be improved. Wireless power transfer would be a fantastic alternative. Engineers have been working on wireless power transmission technologies for decades. Some approaches for wireless power transmission have been developed after extensive investigations. The wireless power system can transmit energy without requiring any mechanical connections.[6]-[10].

Wireless charging is a new technique that may be used to charge a variety of portable consumer electronics devices and battery charging in EVs [9.] It has gained popularity as a result of the removal of direct electrical connections, which makes the system safer and easier to operate.

1.2 CONVERTERS FOR ELECTRIV VEHICLES

The goal of this project is to design and develop converters for EVs applications i.e., to implement wireless power transmission for battery charging using a class-E inverter. Also design and develop Active Clamped Forward Converter, which would be an DC-DC isolated buck derived configuration that is primarily used to extract power from the battery & power up the various other components of electric vehicles such as lights, indicators, and speedometers.

1.3 OBJECTIVE OF THE PRESENTED WORK

The following are the major contributions in this project:

1. Create the mathematical model of class-E resonant inverter and estimate its parameters requirements to the meet the desired design specifications.
2. Conduct a parametric analysis to determine the impact of changing design parameters upon that output performance of class-E resonant inverter.
3. Simulation of class-E resonant inverter in MATLAB/Simulink.
4. To demonstrate concept of impedance matching for WPT.
5. Mathematical calculation for magnetic resonance coupling coils and simulation on MATLAB/Simulink Software.
6. Simulation of rectifier circuit and its implementation for high frequency.
7. Develop a mathematical model for the ACFC and estimate the parameters requirements for desired specifications.

8. Conduct a parametric analysis to determine the impact of variation of design parameters on the output performance characteristics of ACFC.
9. Simulation of ACFC in MATLAB/Simulink Software.
10. Estimation of controller gain] K_p and K_i to get constant output voltage in Active Clamp Forward Converter.

1.4 MOTIVATION

Moving wired equipment from one location to another is quite troublesome. A battery can be used to eliminate the cable & make it portable. However, the battery has several limits, such as the inability to provide power for an extended period of time. It has to be recharged on a regular basis. Medical equipment is often extremely adaptable in terms of mobility and energy usage. As a result, wireless power transmission is the greatest alternative for replacing batteries and making devices more flexible and portable. We may also use it to charge batteries for uninterrupted electricity for equipment that runs for lengthy periods of time. So, using WPT technology, we could run the machines without interruption over an extended amount of time. We have a number of places where we can't install wiring and batteries because they're too little. We may utilize WPT there. Wireless charging, autonomous underwater vehicles, medical equipment, and other applications are among them. Future equipment will be very small in size and very easy to transport from one location to another, even in space and on water, thanks to WPT.
Because the active clamp converter operation when recalibrating the transformer allows products with reduced tolerant voltage to be used for the main switch, and the main switch MOSFET and active clamp converter operate at ZVS to obtain low switching losses, the ACFC described in this document has been widely used for the power supplies requiring high efficiency. ACFC is installed with battery pack to power up various other parts of electric vehicles.

1.5 ORGANIZATION OF THESIS

- Chapter 1 includes a basic introduction, followed by the brief description of Wireless power transfer, battery charging and Active clamp forward converter. It ends with the motivation behind the thesis work.

- Chapter 2 Contains literature survey, brief by describes the power amplifiers, and depict the difference between different types of existing inverter topologies in details. This chapter concludes appropriate selection of inverter components.
- Chapter 3 Refers for details analysis and mathematical modelling of Wireless power transfer that includes modelling and simulation study of class-E resonant inverter, modelling of magnetic resonance coupling.
- Chapter 4 Presents details analysis and mathematical modelling of DC-DC Active clamp forward converter.
- Chapter 5 Conclusions and Recommendation for the Future work.

1.6 SUMMARY

The main goal and purpose of the work present are laid down. The motivation behind selecting the research topic is also described. The scope of the thesis is also briefly mentioned.

CHAPTER 2

LITERATURE REVIEW

2.1 LITERATURE SURVEY

WPT techniques are gaining a lot of attraction these days. WPT technology, which began with the Tesla Coil, is now used in a variety of devices (cellular-phone, laptop, TV, etc.). WPT has been researched in several forms, including self-resonance and inductive coupling systems. However, the majority of research has focused on low-power applications in indoor settings. As a result, WPT for high-power & outdoor applications faces several challenges. My research and development organizations began working on WPT a few years ago. Many of them offered a better system for high-power applications that could deliver maximum power across a wide range; however, this is insufficient for real-world applications. Generally, today's systems are compact and installed to out-door circumstance, therefore there are many problems to solve in WPT system.[11]-[13]

2.2 POWER AMPLIFIER

A power amplifier, often known as an inverter, is a converter that transforms DC/AC electricity. Because inverter circuits may be somewhat complicated, the goal of this technique is to convey a few of the internal workings of inverters rather than becoming bogged down in the finer points. Though the input to that of an inverter circuit would be a dc source, it is not unusual for this derivation to be obtained from an ac source such as a utility ac supply with in context of power electronics. The major source of input power, for example, might be a utility ac voltage input supply which is converted to dc using an ac to dç converter and thereafter reversed back to ac using an inverter. The final output may have a magnitude and/or frequency that is different from the utility supply's input ac [15].

2.3 BRIDGE INVERTER

For a single-phase load, a single-phase square wave VSI provides square-shaped output voltage. The control logic of such inverters is fairly basic, and the switching devices must

work at significantly lower frequencies than switches in other kinds of inverters. The following are the two kinds of bridge inverters:

1. Half-Bridge Inverter
2. Full-Bridge Inverter

These topologies are investigated under idealized circuit circumstances. As a result, the dc input voltage has been expected to be constant and also the switches to be lossless. There are two such legs in a complete bridge topology. Every leg of a inverter is made up of two series-connected electrical switches, as illustrated in the Fig.2.1. Each switch consists of a controlled switch connected to an uncontrolled diode in an anti-parallel configuration. Although these switches may conduct bidirectional current, they only need to block single polarity of voltage. Each leg of inverter contains a single output point for load, which would be the junction-point of switches [16]-[20].

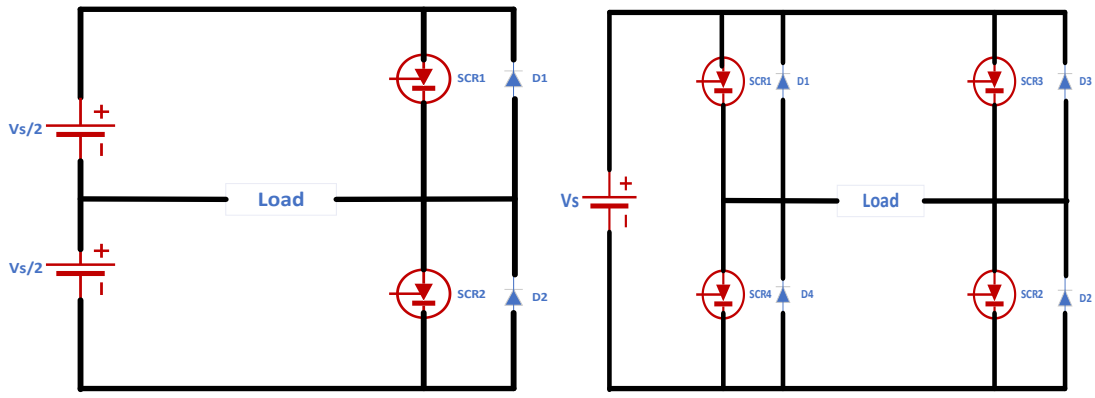

Fig. 2.1 Half-Bridge Inverter in 2.1A and Full-Bridge Inverter in 2.1B.

2.4 RESONANT INVERTER

DC-AC resonant inverters, also called resonant amplifiers. Developments in resonant & quasi-resonant power conversion technology offer alternatives to a competing set of square wave conversion design goals: high efficiency operating at a high switching frequency from a high voltage source. By and large, traditional methods are still in use in the manufacturing world. Emerging resonant technologies, on the other hand, are posing a growing difficulty, owing to their lossless switching benefits. The goal of this thesis is to decipher the subtleties of zvs by analyzing the time intervals as well as the pertinent voltage & current waveforms. Basic resonance topology is shown in **fig. 2.2**.

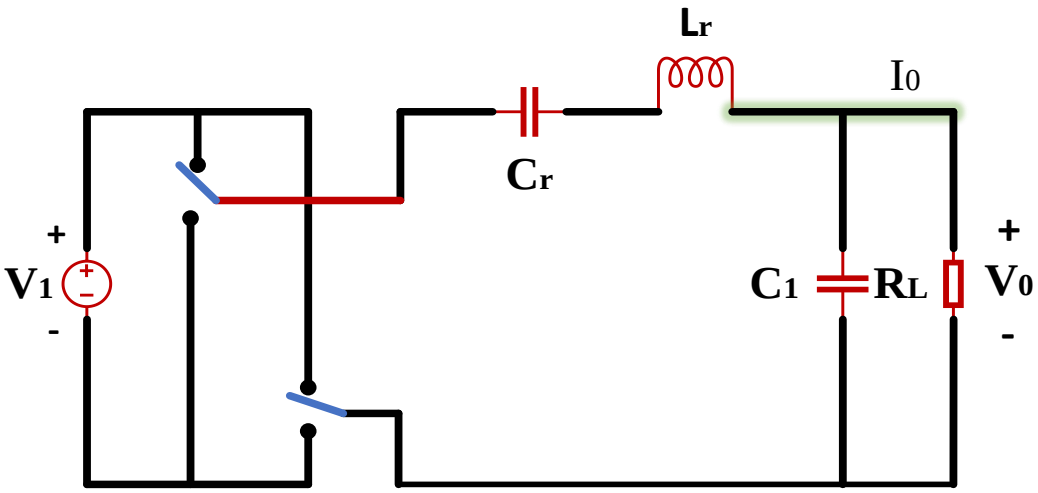

Fig. 2.2 Basic Configuration of Resonant Inverter.

2.4.1 TYPES OF RESONANT IINVERTER

Types of resonant inverter are given below:

1. Class D resonant inverter
    a. Class D Series-Resonant Inverter
    b. Class D Parallel-Resonant Inverter
    c. Class D Series-Parallel-Resonant Inverter
    d. Class D CLL Resonant Inverter
    e. Class D Current-Source-Resonant Inverter
2. Class E inverter
3. Class EF2 inverter

2.5 RECTIFIER AND BATTERY CHARGING

Rectifiers are widely used to transform AC to DC power. To provide this purpose, a rectifier is made up of semiconductor diodes. Full wave, full - wave bridge, and type D rectifiers are examples of rectifiers.

2.5.1 RECTIFIER CIRCUIT

Full wave bridge is used to rectify both half (+ve and -ve) of AC current. Bridge rectifier has several advantages over simple full wave rectifier. It's performance and efficiency

are better than that of the simple full wave rectifier. Voltage stress is low in full bridge-rectifier.

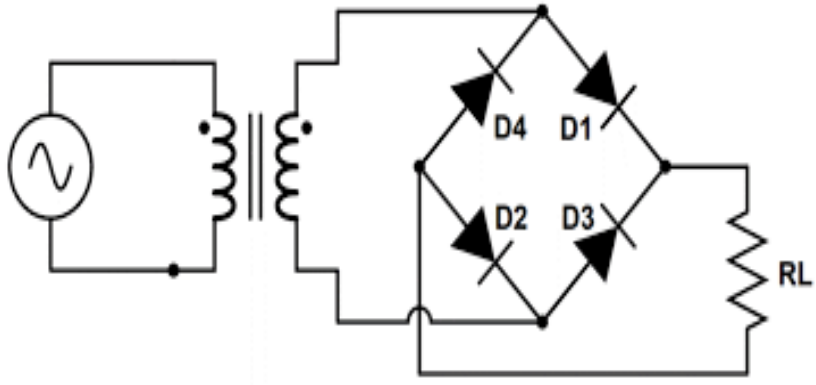

Fig. 2.3 Bridge-Rectifier.

2.5.2 TYPES OF RECTIFIER CIRCUIT

There are two types of rectifiers that are regularly used: Half-wave & full-wave rectifier. Type of rectifier circuits are shown in **fig.2.4**

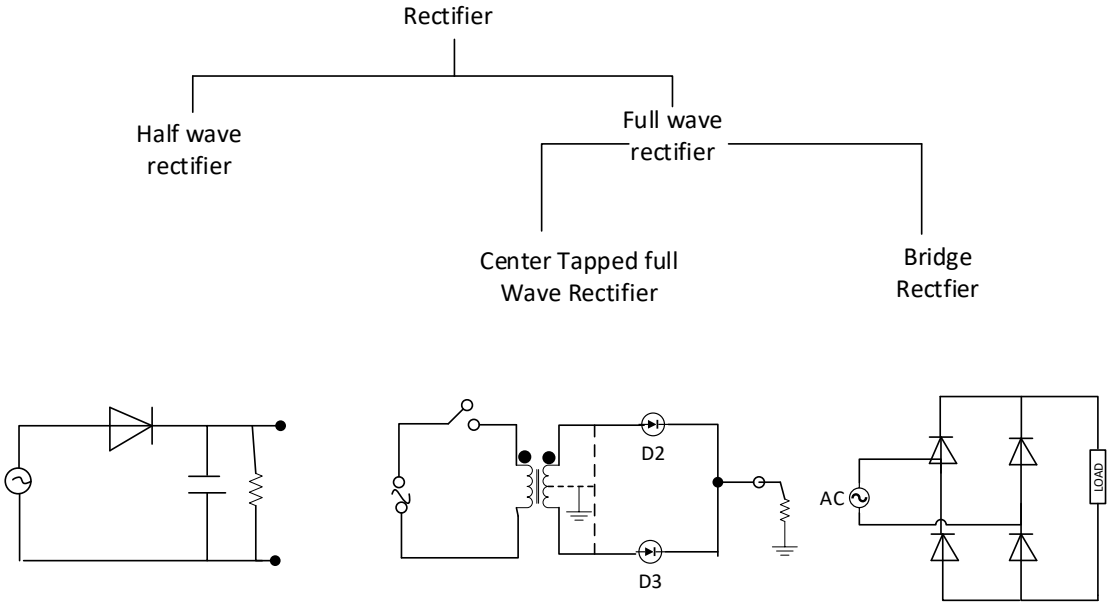

Fig. 2.4 Classification of rectifier.

Half-wave rectifiers have a disadvantage over full-wave rectifiers. Full wave rectifiers are divided into two types: center tapped and bridge rectifiers. How-ever number of devices are required more in bridge rectifier but there are some advantages like; PIV is half in compared to center tapped and transformer utilization factor is higher than the center tapped rectifier.

2.6 TYPES OF BATTERY AND CHARGING TECHNIQUE

Types of battery charging techniques are given below:

1. Conventional Boost Charging.
2. Optimal Boost Charging
3. Pulse Charging
4. Reflex Charging

The charging current must be dispersed after batteries are fully charged. As a result, heat and gases are produced, both are harmful to batteries. The core of successful charging is the ability to identify when the active chemicals have been fully reconstituted and to interrupt this charging process well before harm occurs, all while keeping the cell temperature below safe limits. Detecting and stopping the charge at this cutoff moment is crucial for conserving battery life. When a specified higher voltage limit, also known as the termination voltage, is reached with in simplest of chargers, this occurs. This is especially critical when using fast chargers because the risk of overcharging is higher.

2.6.1 CONVENTIONAL BOOST CHARGING

In the conventional battery charging method, Current and voltage both are varies gradually. Voltage of battery terminal increases and current going into battery is decreases gradually. In this method battery takes lot of time to charge. The current & voltage waveforms are illustrated in **Fig.2.5.**

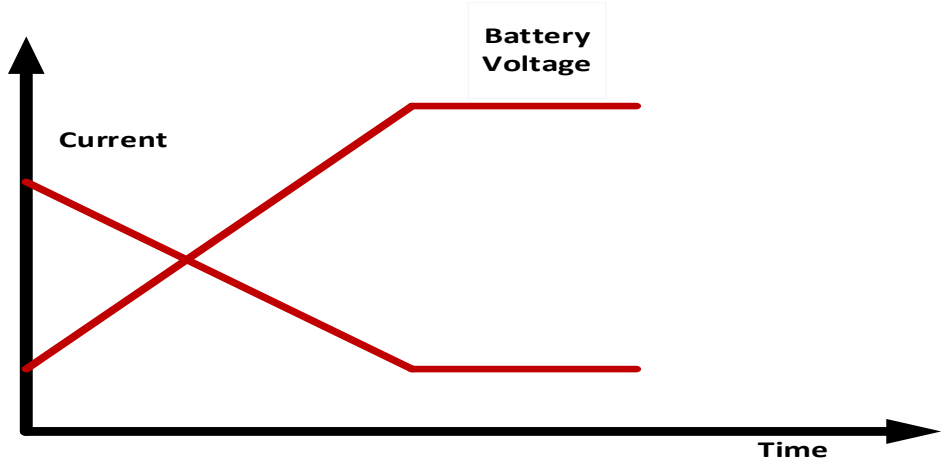

Fig. 2.5 Conventional Battery Charging Waveform.

2.6.2 OPTIMAL BOOST CHARGING

In optimal Boost charging, there are two modes:

1. Constant current mode (CCM)
2. Constant voltage mode (CVM)

The CC & CV modes aid in the proper charging of a battery. It's also a quick-charging method for a battery. But there is a problem that is chemical damage in battery because of constant current supply. CC and CV modes of charging shown in **fig.2.6**.

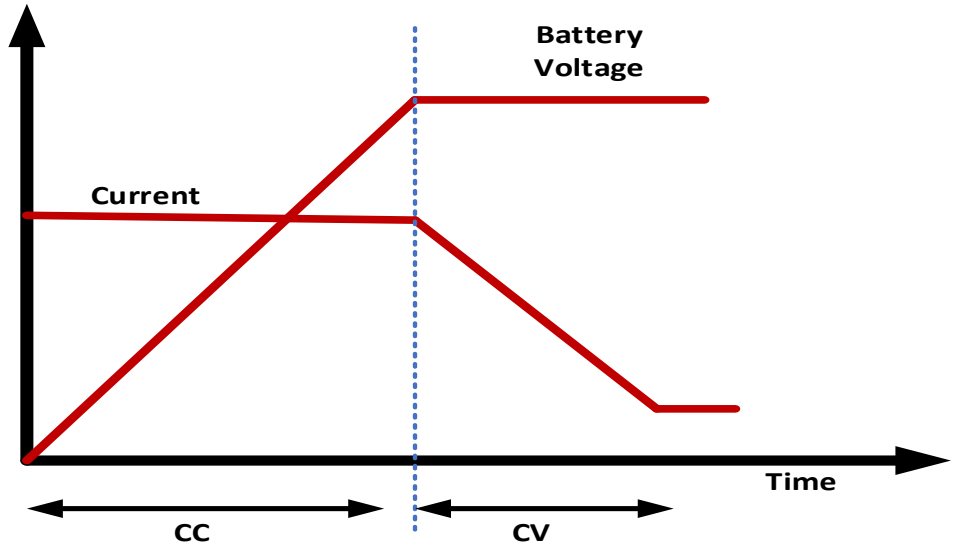

Fig. 2.6 Optimal Battery Charging.

2.6.3 PULSE CHARGING

To overcome the chemical damage pulse charging is introduce this is the modification in optimal battery charging technique. To protect the battery from chemical damage.

The difficulty in developing and deploying a pulsed charging algorithm is reliably identifying and characterizing the parameters that generate the best battery performance. **Fig 2.7** depicts the CC and CV modes. Pulse charge currents have a variety of properties that may be set to various levels, as well as the batteries output performance measures, like as charge and energy efficiency, life span, and charge time, will vary based on the qualities chosen and their levels.

High instantaneous voltages could be provided to the battery without overheating it when pulse charging is used. It thus starts to break down lead-sulfate crystals in a lead-acid battery, prolonging its service life significantly.

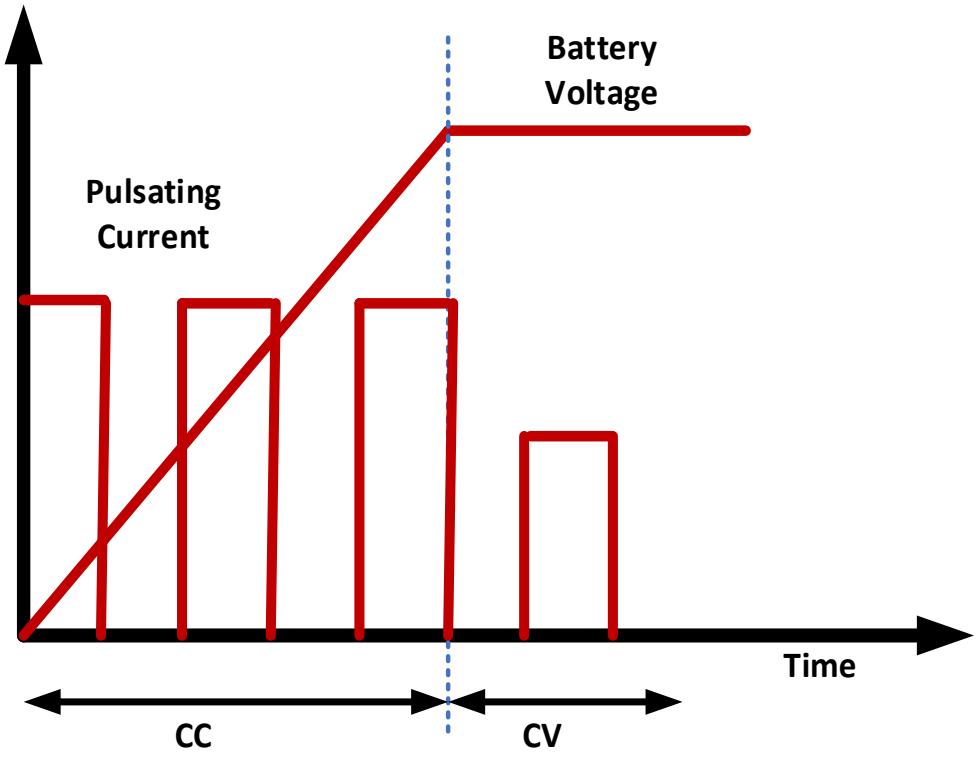

Fig. 2.7 Pulse Charging.

2.6.4 REFLEX CHARGING

Because of the operational savings, enhanced productivity, and safety that fast charging for industrial batteries provides, it is positioned to become a mainstream charging method. Fast charging systems are already humming at production sites and distribution centers all around the world, as users realize the benefits. Reflex charging is a technique of fast battery charging without chemical damage in battery. Current waveform for reflex battery charging is shown in **fig.2.8**

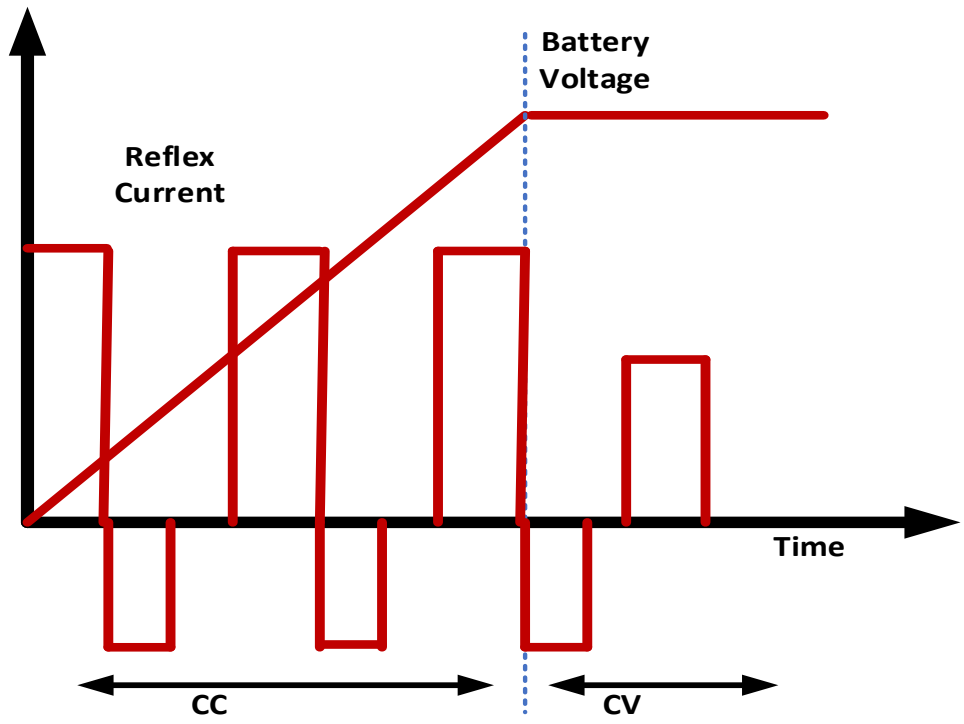

Fig. 2.8 Current in Reflex Charging.

Negative pulse charging, often known as burp charging, is a type of reflex charging. Both positive and negative current pulses are used in this charging procedure. Normal pulse charging is less effective than negative pulse charging.

2.7 CONCLUSION

In this chapter basic topology of inverter and rectifiers are discussed. Different charging methods of battery along with the advantages and disadvantages are also discussed in details.

CHAPTER 3

WIRELESS POWER TRANSFER USING CLASS-E RESONANT INVERTER AND MAGNETIC RESONANCE COUPLING

3.1 INTRODUCTION

WPT allows electrical power to be transferred between a source & a load without the need for physical contact. This includes three parts: DC to AC conversion, wireless power transfer and AC to DC conversion. A high-frequency Class E-inverter is employed in this work, which is working on a single switch resonant phenomenon. Class E-inverter has the advantage of having very low stress across the switch. The size of circuit components like inductors and capacitors is reduced while using high frequency operation. The magnetic resonance coupling_(MRC) is used to enable WPT because it is more efficient for power transfer range over a variable distance in comparison to capacitive and inductive resonant coupling [21]-[23].

WPT is really a novel technology that allows electrical power that will be transferred between the load and source without the use of wires. The purpose of this work is to suggest the usage of a simple and low-cost, electrical power transmission solution in electric vehicles. The many technologies available for WPT and the necessity for a wireless energy transmission system are discussed in the literature. The key difficulty is how to distribute power wirelessly without harming the environment and humans. The WPT is beneficial due to two fundamental battery problems: limited battery life & expensive initial cost. Taking EVs as an example, while many automotive manufacturers promise that their products can travel over 200 kilometers on a single charge, many EV drivers only dare to travel approximately 180 kilometers due to range anxiety. To expand range, EVs must charge regularly or install larger battery packs, both of which introduce additional issues such as cost and weight. The WPT technique is a potential technique for reducing the cost & size of EV batteries, as well as the problem of range and cost. It will be the only way to automate EVs in the future. Battery-powered gadgets may draw

power wirelessly from the electromagnetic field in the air using the WPT technology. This charging system can address the concerns of poor battery life and high initial costs associated with the installation of a huge number of battery packs [24]-[25].

The foundation of this technique is the utilization of magnetic resonance for wireless power transmission in charging applications. Electric power is transported over a short distance using resonance at a frequency of around 100 kHz to charge a battery. Maximum power is transferred through an impedance matching network. Wireless power transfer (WPT) innovation had sparked a lot of interest since it has the potential to revolutionize everyday life and a wide range of businesses. Mobile devices, domestic applications, industrial robots, electric cars, medical instruments, aviation, oil and gas extraction, and soon are just a few of WPT's potential uses [26]-[29].

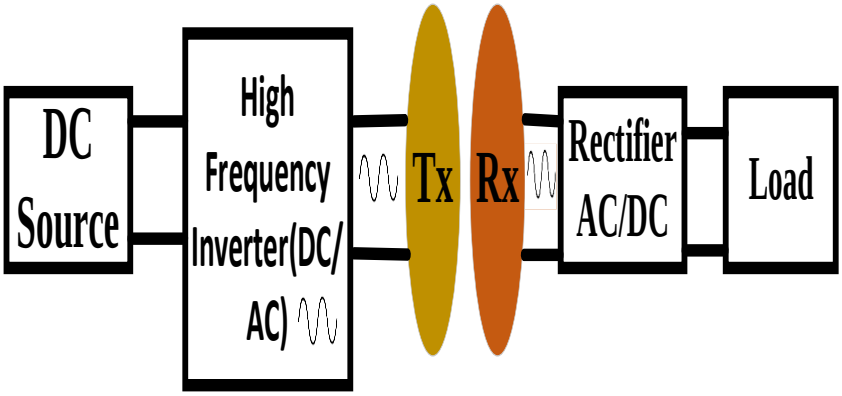

Fig. 3.1 WPT system configuration.

3.2 WIRELESS POWER TRANSFER METHOLOGY

Instead of using wires, the WPT technology may transport power from a power supply to a target through the air. The far-field and near-field transmissions are often used in this innovative energy accessing technology. The energy carrier for far-field WPT might be acoustic, optical, or microwave. The near-field approach takes the use of inductive coupling effect by non-radiative electromagnetic fields, such as magnetic resonance coupling (MRC) processes, which is the focus of this work.

3.2.1 CLASS-E RESONANT INVERTER

Class E DC-AC inverters are characterized into two sub parts i.e., zero-voltage switching_(ZVS) and zero-current switching_(ZCS). The MOS transistor functions as a switch in Class E inverters. Soft-switching inverters include Class E ZVS & Class E

ZCS. A most efficient inverters so far have been Class E ZVS inverters. To get a very high inverter efficiency, the voltage & current waveform of a switch are shifted in time. If a component-values there in resonant circuit are suitably chosen, the switch will turn on at zero voltage. Switching losses were virtually zero since the switch voltage & current waveform would not overlap during switching time periods, resulting in great efficiency.

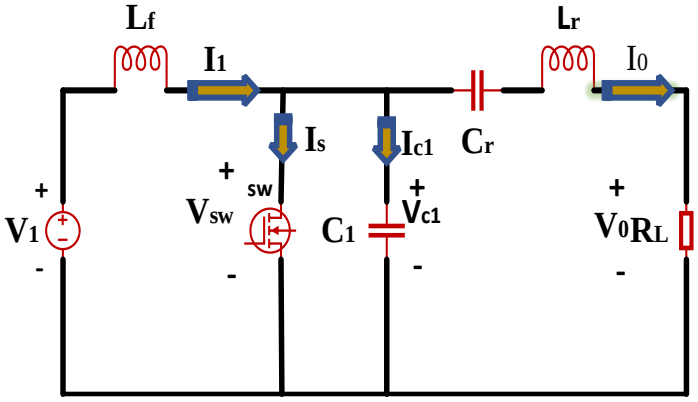

Fig.3.2 Class-E Resonant Inverter Circuit Diagram

3.2.2 CLASS-E ZVS INVERTER DESIGN

The following assumptions are made to construct a class-E inverter that includes the component values of the Class E ZVS inverter illustrated in Fig. 2:

1. The transistor and diode are an ideal switch having zero ON-state resistance, infinite off-state resistance, & zero switching times.
2. The choke inductance_(L_f) being large enough, so that the ac part of the input current is substantially smaller than the DC component.
3. The L_r-C_r-R_L series-resonant circuit's loaded Q_L is high enough to provide sinusoidal current_(I_0) across the resonant circuit.

From the Waveforms of Current & Voltage

The current into the series-resonant circuits is sinusoidal, and it may be written as

$$I_0 = I_m \sin(wt + \phi) \tag{3.1}$$

Where I_M is the maximum amplitude and ϕ is current's beginning phase

$$I_s + I_{c1} = I_1 - I_0 = I_1 - I_m \sin(wt + \phi) \tag{3.2}$$

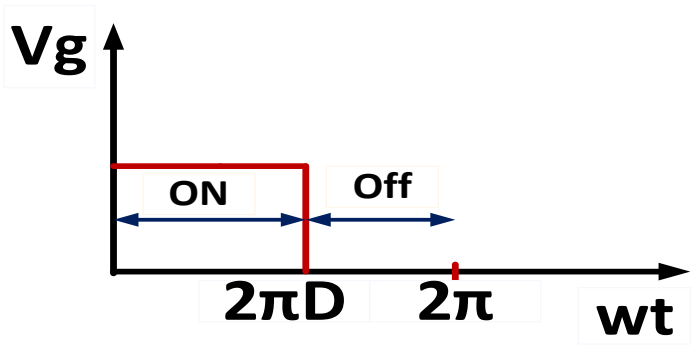

Fig.3.3 Gate Pulse for switch ON/OFF

where, D is Duty Ratio of switch,

For the duration of the period $0 \le wt \le 2\pi D$ (Switch ON)

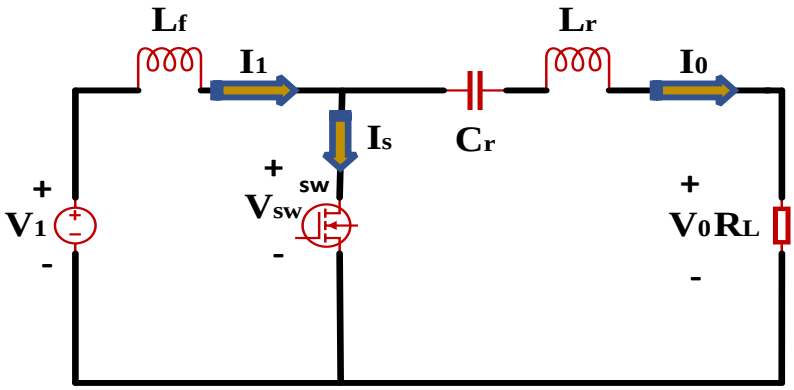

Fig.3.4 Resonant Inverter (Class E) Circuit Diagram

(Switch ON)

$$I_s = \begin{cases} I_1 - I_m \sin(wt + \phi) & 0 \le wt \le 2\pi D \\ 0 & 2\pi D \le wt \le 2\pi \end{cases} \quad (3.3)$$

For the time interval $2\pi D \le wt \le 2\pi$ (Switch OFF)

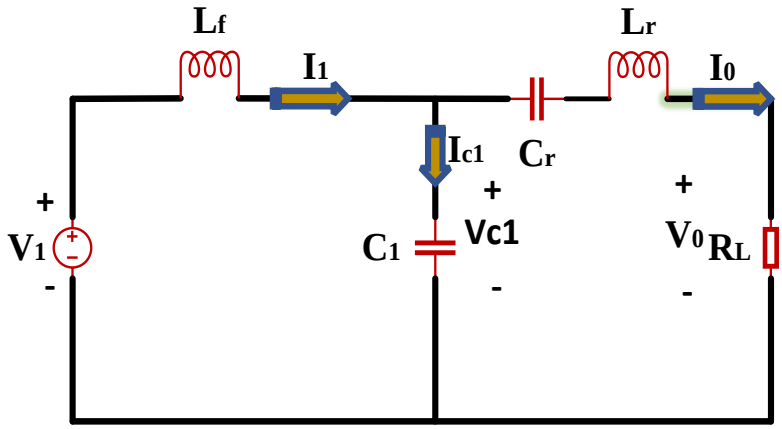

Fig.3.5 Resonant Inverter (Class E) Circuit Diagram

(Switch OFF)

Because the switch is turned off, i.e Is=0, the current through shunt capacitors_C1 is equal to

$$I_{c1}=\begin{cases}0 & 0\le wt\le 2\pi D\\ I_1-I_m\sin(wt+\phi) & 2\pi D\le wt\le 2\pi\end{cases} \tag{3.4}$$

The voltage to across s/w and shunt capacitor is

$$V_{sw}=\frac{1}{wC_1}\int_{2\pi D}^{2\pi} I_{c1}d(wt)$$

$$=\left\{\frac{1}{wC_1}\left[I_1(wt-2\pi D)+I_m[\cos(wt+\phi)-\cos(2\pi D+\phi)\right]\right. \tag{3.5}$$

Substituting condition $V_{sw}(wt=2\pi)=0$

$$I_m=I_1\frac{2\pi(1-D)}{\cos(2\pi D+\phi)-\cos(\phi)} \tag{3.6}$$

Putting value of I_m in eq. (3.3)

$$\frac{I_s}{I_1}=\begin{cases}1-\dfrac{2\pi(1-D)\sin(wt+\phi)}{\cos(2\pi D+\phi)-\cos(\phi)} & 0\le wt\le 2\pi D\\ 0 & 2\pi D\le wt\le 2\pi\end{cases} \tag{3.7}$$

Putting value of I_M in eq. (3.4)

$$\frac{I_{c1}}{I_1}=\begin{cases}0 & 0\le wt\le 2\pi D\\ 1-\dfrac{2\pi(1-D)\sin(wt+\phi)}{\cos(2\pi D+\phi)-\cos(\phi)} & 2\pi D\le wt\le 2\pi\end{cases} \tag{3.8}$$

Putting value of I_m from eq. (3.6) into eq. (3.5)

$$V_{sw}=\frac{I_1}{wC_1}\left\{(wt-2\pi D)+\frac{2\pi(1-D)[\cos(wt+\phi)-\cos(2\pi D+\phi)]}{\cos(2\pi D+\phi)-\cos(\phi)}\right\} \tag{3.9}$$

Using the condition

$$\frac{dV_{sw}}{dwt}=0$$

$$\tan(\phi)=\frac{\cos(2\pi D)-1}{2\pi(1-D)+\sin(2\pi D)} \tag{3.10}$$

DC input voltage is given by

$$V_1=\frac{1}{2\pi}\int_{2\pi D}^{2\pi} V_{sw}d(wt)$$

$$V_1 = \frac{I_1}{wC_1}\left\{\frac{(1-D)[\pi(1-D)\cos(\pi D)+\sin(\pi D)]}{\tan(\pi D+\phi)\sin(\pi D)}\right\} \tag{3.11}$$

The Class E inverter's DC input resistance is

$$R_{dc} = \frac{V_1}{I_1} = \frac{1}{wC_1}\left\{\frac{(1-D)[\pi(1-D)\cos(\pi D)+\sin(\pi D)]}{\tan(\pi D+\phi)\sin(\pi D)}\right\} \tag{3.12}$$

The voltage amplitude across load R_0 is calculated as

$$V_0 = \frac{1}{\pi}\int_{2\pi D}^{2\pi} V_{sw}\sin(wt+\phi)\,d(wt)$$

$$V_0 = \frac{2\sin(\pi D)\sin(\pi D+\phi)}{\pi(1-D)}V_1 \tag{3.13}$$

Output Power for class E inverter is

$$P_0 = \frac{V_0^2}{2R_L} = \frac{2\sin^2(\pi D)\sin^2(\pi D+\phi)V_1}{\pi^2(1-D)^2 R_L} \tag{3.14}$$

Parameter value for class E inverter at duty ratio $(D) = 0.5$

$$\tan(\phi) = \frac{\cos(2\pi D)-1}{2\pi(1-D)+\sin(2\pi D)} = \frac{-2}{\pi} \tag{3.15}$$

$$P_0 = \frac{V_0^2}{2R_L} = \frac{2\sin^2(\pi D)\sin^2(\pi D+\phi)V_1^2}{\pi^2(1-D)^2 R_L} = \frac{8}{\pi^2+4}\frac{V_1^2}{R_L} \tag{3.16}$$

$$wC_1R_L = \frac{8}{\pi(\pi^2+4)} = 0.1836 \tag{3.17}$$

$$Q_L = \frac{wL_r}{R_L} \tag{3.18}$$

$$\frac{1}{wC_rR_L} = Q_L - \frac{\pi(\pi^2-4)}{16} \tag{3.19}$$

3.3 DESIGN OF COUPLING COILS

Magnetic resonance coupling consists of two coils that are transmitting and receiving coils. Magnetic resonance coupling works by transmitting power between two coils working at same resonant frequency using a high-frequency alternating magnetic field. The coils could be loosely connected, but energy transmission for several centimetres requires a high Q factor.

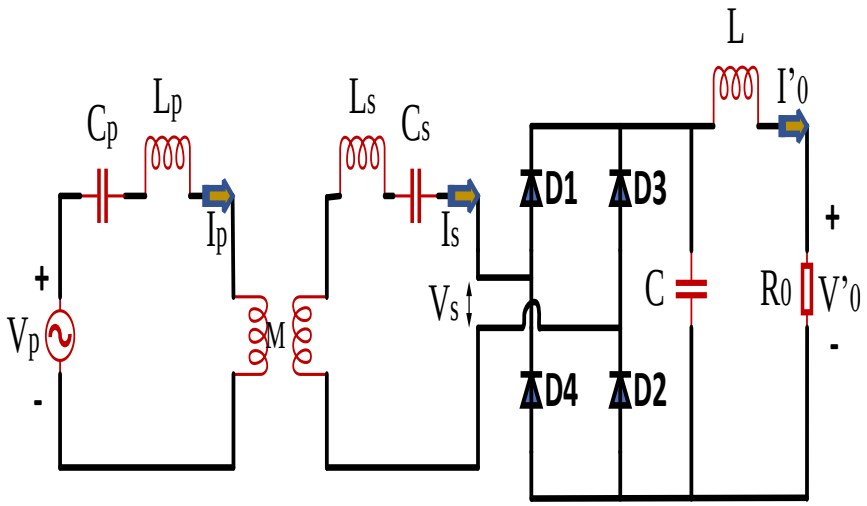

Fig. 3.6 Block diagram of MRC

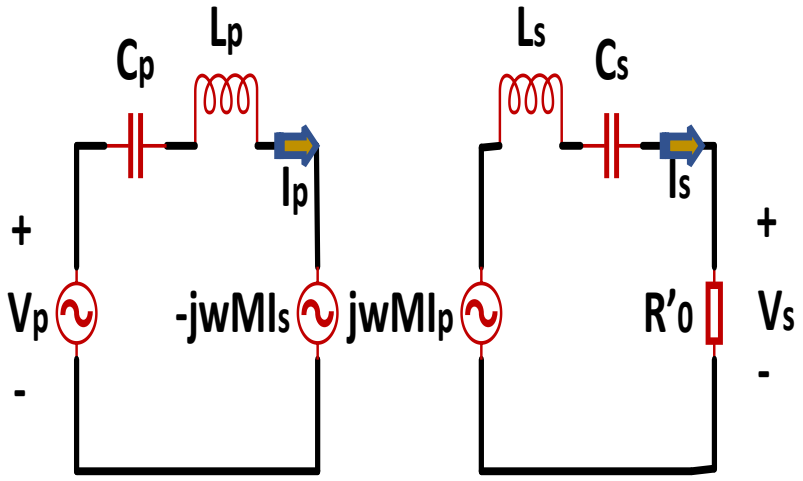

Fig. 3.7 Magnetic Resonance Coupling

$$Z_pI_p - jwMI_s = V_P \tag{3.20}$$

$$Z_sI_s = jwI_p \tag{3.21}$$

where, V_p is voltage at transmitting Coil, I_p is current through transmitting Coil, M mutual inductance exists between the two coils, the voltage received at receiving coil is denoted by V_s, I_S is the current through receiving coil, R_0 is the output impedance, R'_0 is equivalent output impedance.

$$Z_p = jwL_p + \frac{1}{jwC_p} \tag{3.22}$$

$$Z_s = jwL_s + \frac{1}{jwC_s} + R'_0 \tag{3.23}$$

$$R_0 = \frac{V'^2_0}{P_0} \tag{3.24}$$

$$R'_0 = \frac{8R_0}{\pi^2} \tag{3.25}$$

L_P, C_P denote transmitting coil inductance and capacitance linked in series with coils, respectively, and L_S, C_S denote receiving coil inductance and capacitance series connected with receiving coil.

Multiplying eq. (3.20) by Z_s and eq. (3.21) by jwM

$$Z_pZ_sI_p - jwMZ_sI_s = V_pZ_s \tag{3.26}$$

$$jwMZ_sI_s + w^2M^2I_p = 0 \tag{3.27}$$

Adding eq. (3.26) and eq. (3.27) and dividing it by Z_s we get

$$Z_p + \frac{w^2M^2}{Z_s} = \frac{V_p}{I_p} \tag{3.28}$$

$$Z_r = \frac{w^2M^2}{Z_s} = \frac{w^2M^2}{jwL_s + \frac{1}{jwC_s} + R'_0} \tag{3.29}$$

where, Z_r is reflected impedance of receiving coil side to transmitting coil side and $Z_{in} = \frac{V_p}{I_p}$ is the impedance as viewed from transmitting coil side.

At resonance frequency (W_0), the inductor's inductive reactance equals to capacitive's capacitive reactance.

$$jw_0L_s - \frac{j}{w_0C_s} = 0 \tag{3.30}$$

$$C_s = \frac{1}{L_sw_0^2} \tag{3.31}$$

$$Z_r = \frac{w_0^2M^2}{R'_0} \tag{3.32}$$

$$Z_{in} = jw_0L_p + \frac{1}{jw_0C_p} + \frac{w_0^2M^2}{R'_0} \tag{3.33}$$

The imaginary component of input impedance becomes zero at resonance frequency.

$$C_p = \frac{1}{L_pw_0^2} \tag{3.34}$$

The receiving coil sides circuit becomes pure resistive in resonance, the reactance parameters neutralize one another and the, one may obtain

$$M = I_{srms}\frac{R'_0}{W_0\, I_{prms}} \tag{3.35}$$

where, I_{prms} and I_{srms} are the transmitting and receiving coil RMS current.

$$L_s = \frac{Q_L R'_0}{w_0} \tag{3.36}$$

$$K_c = \frac{\sqrt{1 - \frac{1}{4Q_L^2}}}{Q_L} \tag{3.37}$$

where, K_c is coefficient of coupling.

$$L_p = \frac{M^2}{L_s K_c^2} \tag{3.38}$$

3.4 SIMULATION RESULTS AND DISCUSSION

3.4.1 SIMULATION RESULTS

In this study a WPT scheme for transfer of about 85.5W power at transmitting end voltage of voltage V1=35Vand receiving end voltage $V'_0 = 23V$ is designed and/or simulated in MATLAB/Simulink. The design specifications of WPT scheme is shown in Table5.1 and Table5.2. A MATLAB model of the proposed scheme is developed for simulation.

3.4.2 PARAMETER & COMPONENT VALUE

Table 3.1 WPT Design specification

Parameter	Value
Input voltage (V_1)	35V
Input Power (P_1)	100W
Switching frequency (f)	100KHz
Resonant frequency (f_0)	93.639 KHz
Output voltage (V'_0)	23.18V
Output power (P_0)	85.47W
Efficiency (η)	85.74%

Table 3.2 Component value developed for WPT scheme

Components	Values
L_f	485.436μH
C_1	41.74nF
C_r	25.69nF
L_r	112.45μH
R_L	7.06Ω
C_p	21.7nF
L_p	116.68μH
C_s	31.416nF
L_s	80.628μH
M	9.68μH
K_c	0.1
C	6.57μF
L	42.98μH
R_0	6.25Ω

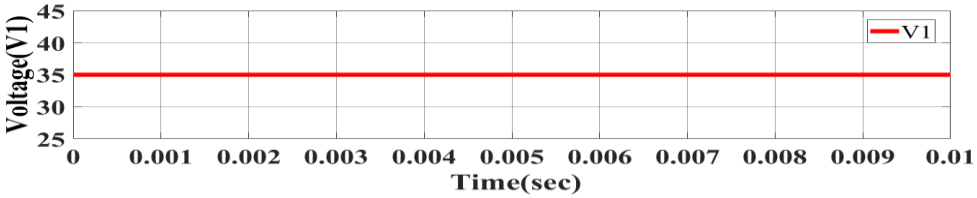

Fig. 3.8: Supply Voltage

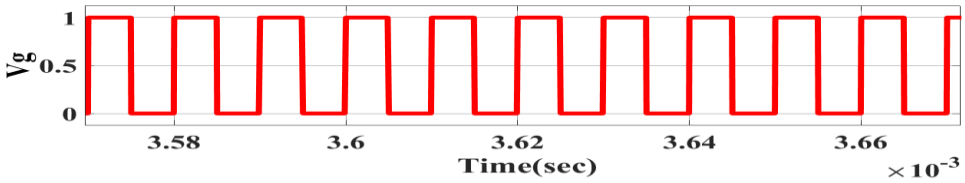

Fig. 3.9: Switching Pulse

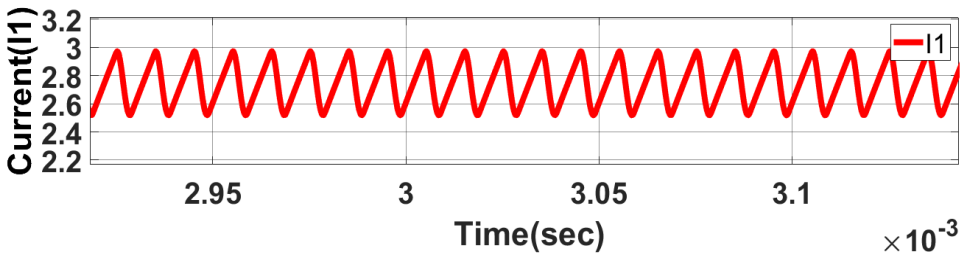

Fig. 3.10: Input Current

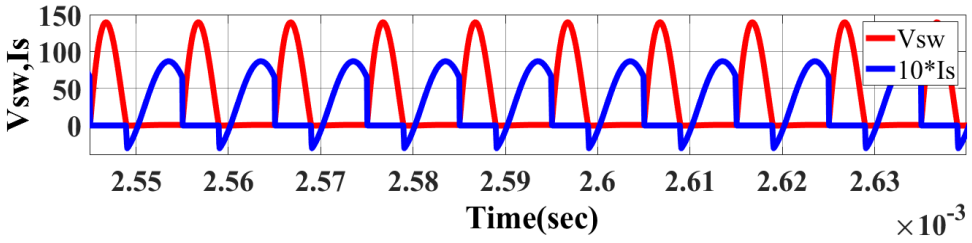

Fig. 3.11: Zero Voltage Switching

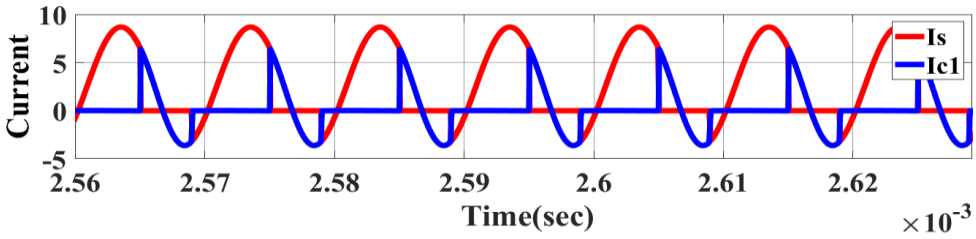

Fig. 3.12: Switch Current and Shunt Capacitor Current

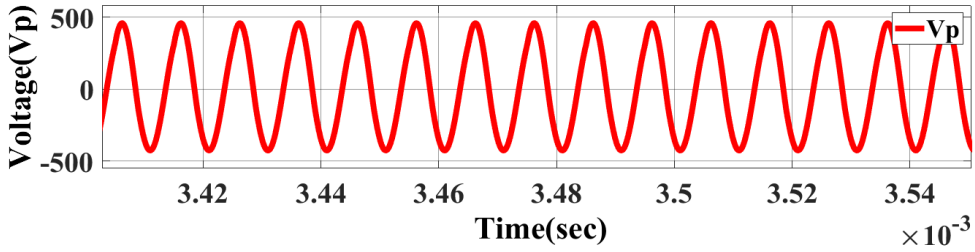

Fig. 3.13: Voltage of Transmitting Coil

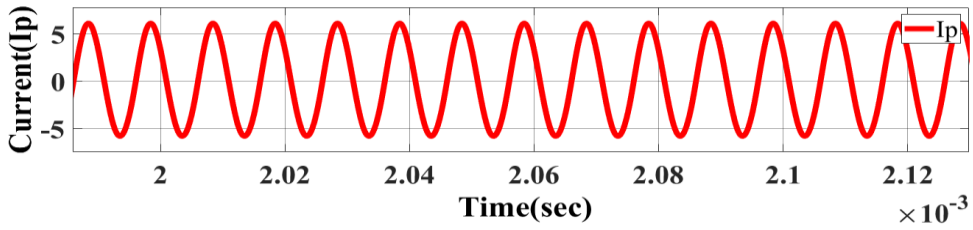

Fig. 3.14: Current of Transmitting Coil

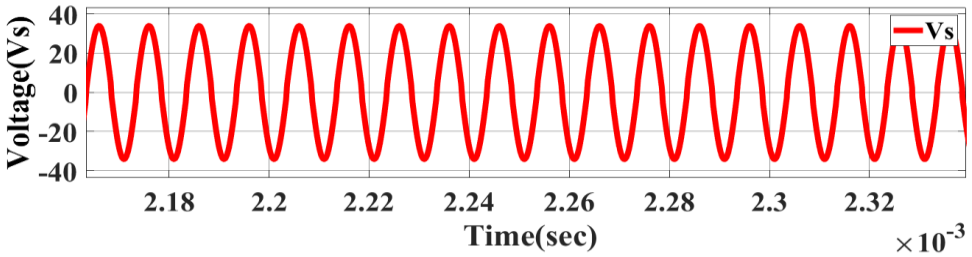

Fig. 3.15: Voltage of Receiving Coil

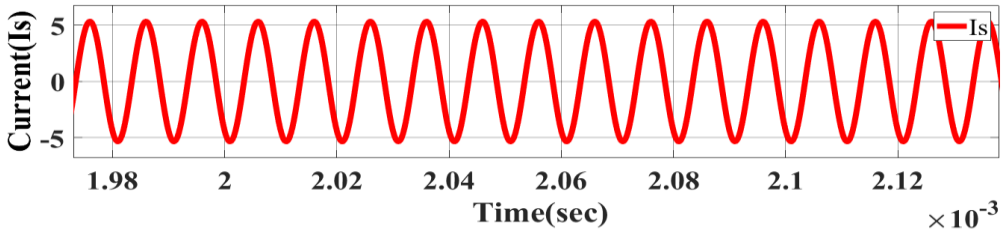

Fig. 3.16: Current of Receiving Coil

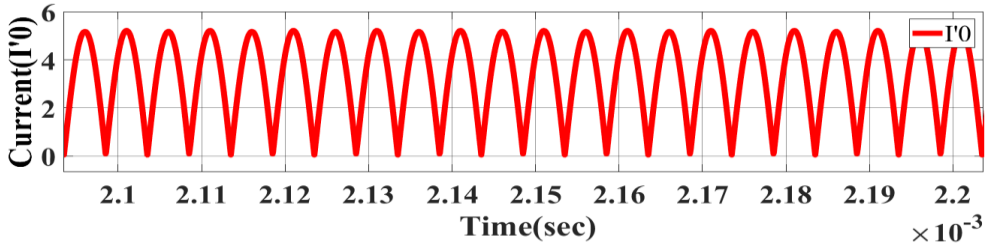

Fig.3.17: Output Current Without Output Filter

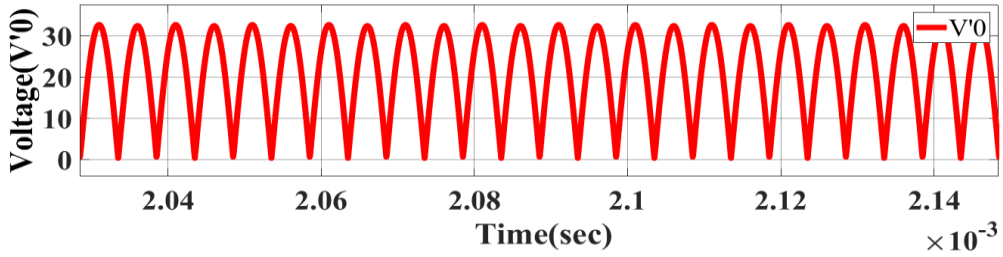

Fig. 3.18: Output Voltage Without Output Filter

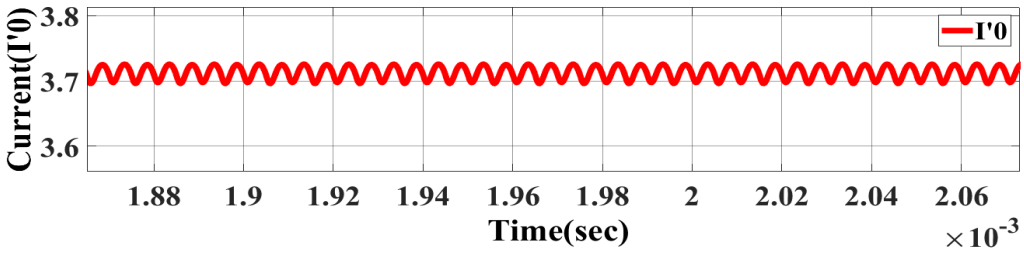

Fig. 3.19: Output Current with Output Filter

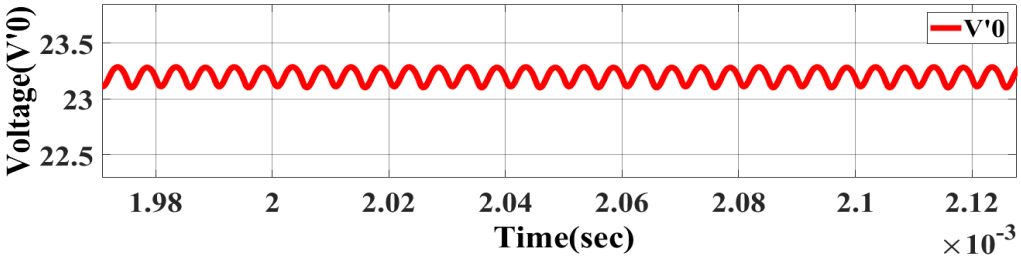

Fig. 3.20: Output Voltage with Output Filter

3.5 RESULT AND DISCUSSION

A 2-coil WPT system's circuit modelling has been introduced. The link between the circuit characteristics, coupling coefficients energy transfer, and efficiency is investigated using circuit theory. The WPT prototype is powered by a 35V, 2.79A Power supply. As indicated in **Fig.3.13 to Fig.3.16**, the resonance frequencies of the Receiver and Transmitter coil are well matched. The applied input voltage and input current are DC and the choke inductance_(Lf) is used to reduce the ripple in input current, higher is the value of choke inductance_(Lf) lower will be the ripple in input current. Output voltage and output current are pulsating DC obtained when high frequency AC is passed through diode rectifier shown in **Fig.3.17 to Fig3.18**. To smooth output current and voltage, L-C filter is designed for 5 % ripple in o/p current and voltage as illustrated in **Fig.3.19 to Fig.3.20**. **Fig.3.11**, shows the ZVS across the switch. ZVS is used to decrease switching losses with in switch & boost the inverter's efficiency. The Switch Current & Shunt Capacitance_(C1) Current are shown in **Fig.3.12**. Because of the short-circuit, voltage all across switch & shunt capacitor_(C1) is zero while the switch is ON, however when the switch has been off, current through shunt capacitor_(C1) is accountable for voltage build-up across the switch.

3.6 CONCLUSIONS

Moving wired equipment from one location to another is quite troublesome. A battery can be used to eliminate the cable & make it portable. However, the battery has several limits, such as the inability that provide power for an extended period of time. It has to be recharged on a regular basis. Medical equipment is often extremely adaptable in terms of mobility and energy usage. As a result, wireless power transmission is the greatest alternative for replacing batteries and making devices more flexible and portable. We may also use it to charge batteries for uninterrupted electricity for equipment that runs for lengthy periods of time. Therefor WPT technology, enables machines operation without interruption for a long amount of time. There are number of places where it is not possible to install wiring and batteries because they're too little. We may utilise WPT there. Wireless battery charging is one of our many applications. Medical equipment, autonomous undersea vehicle, etc. Future equipment will be very small in size and very easy to transport from one location to another, even in space and on water.

The ZVS or zero derivative voltage switching_(ZVDS) approaches are provided in this study for Class E resonant inverter based wireless power transmission running at extremely high frequency (100 kHz). Switching losses are avoided and circuit efficiency is enhanced by running the inverter at ZVS or zero derivative voltage switching_(ZVDS). Further this high frequency inverter is used for WPT application with the help of magnetic resonance coupling_(MRC). Implementation of WPT scheme for supply voltage of 30V and input power of 100W, output voltage 23.18V and output power of 85.47W and overall efficiency of the system 85.47% is designed and demonstrated through simulation study in MATLAB/Simulink.

CHAPTER-4

ACTIVE CLAMP FORWARD CONVERTER FOR ELECTRIC VEHICLE APPLICATIONS

4.1 INTRODUCTION

A buck-derived converter topology with transformer isolation is used in the ACFC. For low-power applications, the ACFC is a common choice for single or multiple output power supply. Active clamp forward converters are smaller and more efficient than passive clamp forward converter. In forward converter transformer's are utilised to accomplish circuit isolation and energy transformation from primary side to secondary side, as well as to reset the transformer's magnetising current using the active clamp approach. While there are a variety of approaches for accomplishing transformer reset, the active clamp approach is both simple and effective. ZVS (zero voltage switching), decreased switch voltage stress, wider duty cycle range, and reduced EMI (electro-magnetic interference) are just a few of the benefits of active switching. One of the constraints of the active clamp is the requirement for a precise duty clamp. Increased duty cycle, if not limited to a maximum amount, might cause transformer saturation or additional voltage stress on the main switch, both of which will be dangerous. Another constraint is the requirement for sophisticated control to synchronize delay timing between the active clamp and primary switch gate drive. When the switch_(S_M) i.e., main switch ON, its voltage emerges across the primary winding of transformer, causing the magnetizing current_(I_M) to increase linearly and reaches to its maximum positive peak value. For periodic voltage, current functioning of transformer circuit, this established magnetizing current must be reset when the switch_(S_M) is OFF. At the end of every switching phase, the magnetizing current/flux in core should revert to its initial value. If the magnetizing current/flux will not revert to its initial state at the conclusion of each switching phase, the magnetizing current_(I_M) will continue to rise, leading to transformer saturation. By using an active clamp converter, the overall efficiency of the circuit is considerably increased. A variety of ways have been developed to reduce switching losses and increase system's efficiency. With the help of clamp switch_(S_{CL})

and clamp capacitor_(CCL), the active-clamp approach has been developed to collect the excess stored energy inside leakage inductance_(LL) and decrease current, voltage stress of switch_(SM). The active clamp approach uses a normal pulse width modulation_(PWM) system to transmit power and the switch is switched on at ZVS utilizing transformers leakage-inductance_(LL) and parasitic-capacitance and/or switch-output capacitance_(CDS).[29]-[35]

To show ZVS and enhanced efficiency, an ACFC-ZVS converter is built and implemented in MATLAB/Simulink in this study. A complete analysis of system and design approach, and the creation of a 488.6W ACFC zero voltage switching_(ZVS) converter is presented. Using clamp switch_(SCL), clamping capacitor_(CCL), and resonant circuit, the ACFC circuit will reset the surge energy held in leaky inductance and the main-switch voltage-stress is also decreased. To analyse the performance characteristics of the ACFC zero voltage switching_(ZVS) converter, the circuit operation for closed loop system is simulated in MATLAB/Simulink and results for 488.6W prototype circuit with DC link voltage of 80-l20V and output voltage_(V0) of 14V at operating frequency_(Fs) of 250kHz are illustrated through relevant waveforms. The active clamp forward converter's uses include auxiliary power supply for electric cars.

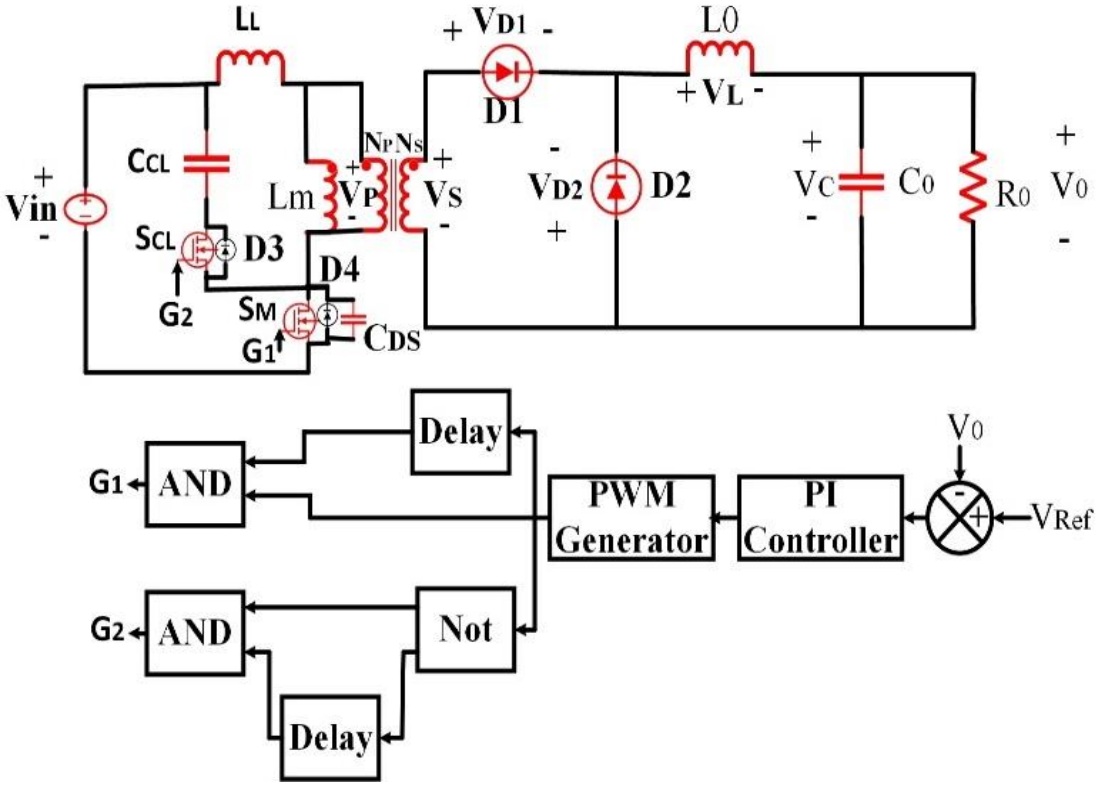

Fig. 4.1 ACFC Circuit Diagram.

4.2 CIRCUIT DESCRIPTION AND ANALYSIS

The ACFC circuit is illustrated in **Fig4.1**. The clamp switch_(S_{CL}) and clamping capacitor_(C_{CL}) in the active clamped circuit are used to reset the magnetising flux of transformer and absorb the surplus energy created by the leakage-inductance_(L_L) to reduce voltage stress on the main-switch_(S_M). To accomplish ZVS functioning for the main switch, the drain_source capacitance_(C_{DS}) and leakage inductance_(L_L) are in resonant_(S_M). The magnetizating inductance is stated as_(L_m). The drain_source capacitance_(C_{DS}) is equal to the parasitic capacitance of the switch_(S_M) i.e. main switch and the switch_(S_{CL}) i.e., clamp switch combined in parallel. The converter makes the following assumptions for circuit analysis.

- The drain-source capacitance_(C_{DS}) should be smaller compared to the clamp capacitance_(C_{CL}).
- The capacitance_C_0 is big enough to maintain an approximately constant steady output voltage.
- The inductance(L_0) of the secondary side filter is large enough so that approximately constant current flow through it.
- The magnetising inductance(L_m) must be greater than leakage inductance (L_L).
- Transformer's turn ratio $n=\frac{N_P}{N_S}$
- Zero voltage switching (ZVS) is accomplished when the inductive energy is larger enough than the energy stored in capacitor of the drain-source capacitance (C_{DS}).

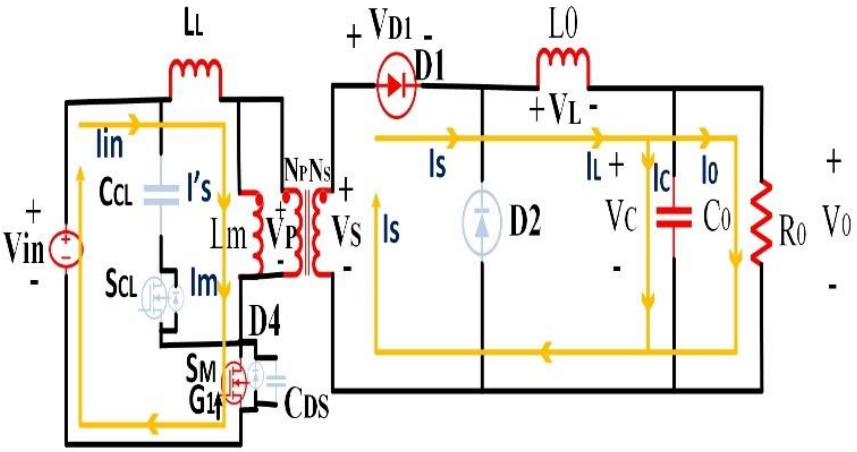

Fig.4.2 Circuit diagram of ACFC, switch (S_M) ON and Switch (S_{SC}) OFF

Mode I:

Power is transferred to the secondary side of transformer in this-mode of operation, as illustrated in **fig.4.2**. The magnetising current_(I_m) of transformer is added to reflected secondary current_(I's) to generate the input current_(I_{in}) and flows via the channel resistance of the switch_(S_M). On the secondary side, forward bias causes diode_(D1) to be ON, while reverse bias causes diode_(D2) to be OFF. The supply voltage is the voltage that appears across the magnetising inductance (V_{in}).

$$I_{in}=I_m+I'_s \tag{4.1}$$

Voltage across magnetising inductance L_m is

$$V_{Lm}=V_{in}=L_m\frac{dI_m}{dt} \tag{4.2}$$

$$\Delta I_m=\frac{DV_{in}}{F_sL_m} \tag{4.3}$$

Voltage across the output inductor L_0 is

$$V_{L0}=V_s-V_0=V_{in}\frac{N_S}{N_P}-V_0 \tag{4.4}$$

$$\Delta I_{L0}=\frac{(V_{in}\frac{N_S}{N_P}-V_0)D}{F_sL_0} \tag{5.5}$$

where V_{Lm} is the voltage of magnetising inductance voltage, V_{L0} will be the voltage across output inductor, D will be the duty cycle, Fs is switching frequency.

Eq. (4.2)- (4.5) show that current through magnetising inductance (L_m) and output inductance inductance (L_0) increases linearly when the switch (S_M) is ON.

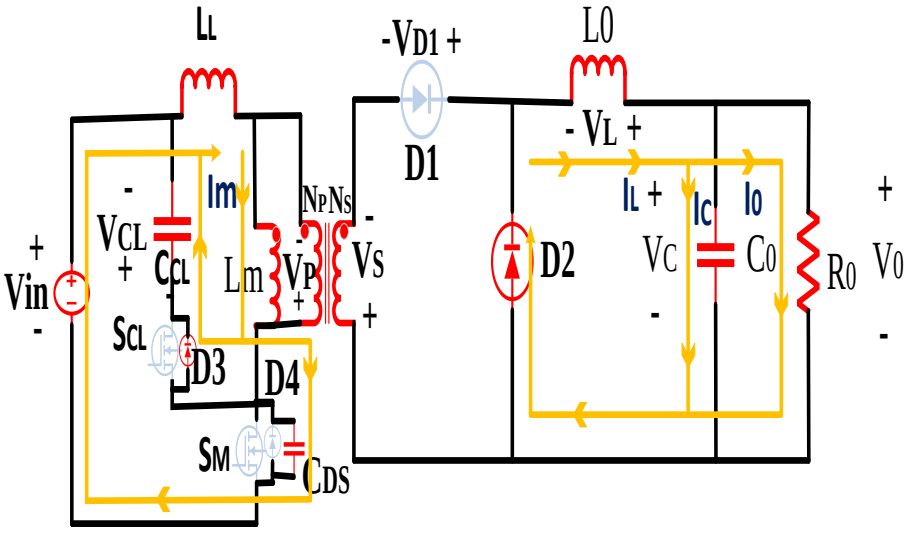

Fig. 4.3 ACFC Circuit when switch (SM) OFF, Switch (SSC) OFF

Mode II:

In this mode of operation, switch_(S_M) is switched off, the primary current_(I_P) continues to charge up the main switch's drain to source capacitor_(C_{DS}), before being diverted through the body-diode_(D3) of clamp-switch and charging clamp-capacitor_(C_{CL}), as illustrated in **Fig.4.3**. Because the secondary side load current (I_0) is freewheeling, there will be no reflected primary current, hence only transformer magnetising current_(I_m) is flowing through D3. As a result, the clamp switch _(D3) body-diode's conduction loss is minimal, and the circumstances are established for clamp switch_(S_{CL}) to turn on under ZVS. The resonant period is the duration between turning-off the switch_(S_M) and turning on the switch_(S_{CL}). Diode_(D1) is off on the secondary side because the transformer secondary applies reverse voltage across it, causing diode_(D2) to conduct and the load current to freewheel through it. Conduction losses of D1 and D2 can be a significant component to overall power loss in high current applications, and are frequently one of the limiting considerations for higher frequency operation.

Voltage across the output inductor L_0 is

$$V_{L0}=-V_0 \tag{4.6}$$

$$\Delta I_{L0}=\frac{-V_0(1-D)}{F_s L_0} \tag{4.7}$$

Eq.(4.7) show that, current through the output inductor decreases linearly when switch S_M,diode D1 is off and D2 is ON.

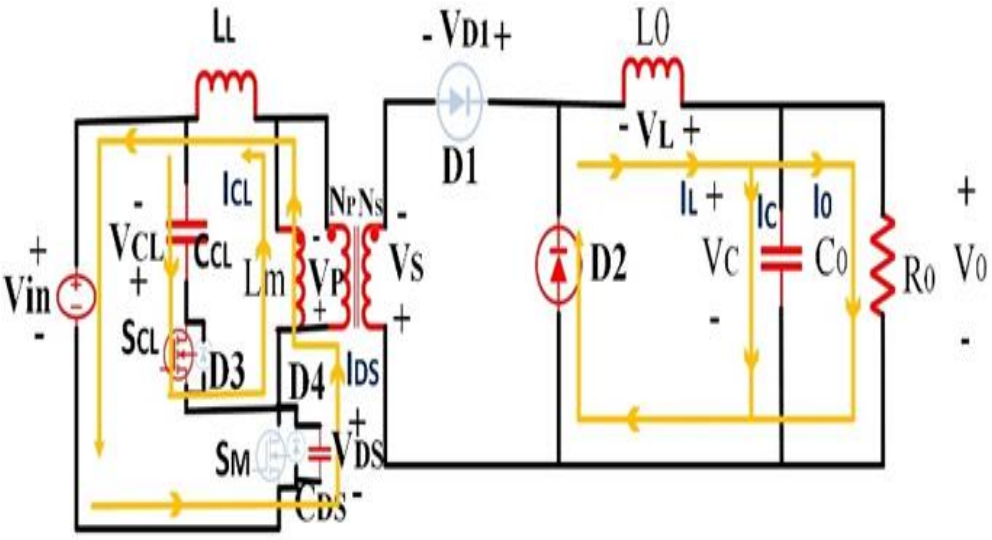

Fig. 4.4 ACFC Circuit when switch (S_M) OFF and Switch (S_{SC}) ON

Mode III:

This is the condition of active clamping, in which the primary side winding of the transformer is reset. Regardless of the fact that the primary current seems to reverse almost instantly in **Fig.4.4**, the change from positive to negative current flow is smooth. The switch_(S_{CL}) is now completely ON, the voltage appear across transformer primary side is the difference of clamp-capacitor voltage_(V_{CL}) and supply voltage_(V_{in}). The clamp capacitor_(C_{CL}) and drain voltage_(V_{DS}) started to fall, while the magnetising current_(I_m) started to rise in the opposite direction. On the other-hand, the diode_(D2) on the secondary side of the transformer, which is carrying entire load current, does have a large conduction loss.

Mode IV:

In this mode of operation, under ZVS, the clamp switch_(S_{CL}) is switched OFF. The main switch drain-to-source capacitance_(C_{DS}) and transformer magnetising current_(I_m) continue to discharge their energy to the supply voltage_(V_{in}), as illustrated in **Fig.4.5**. The magnetising current goes via the main switch's body diode once the C_{DS} is discharged. After then, the switch_(S_M) is then switched ON.

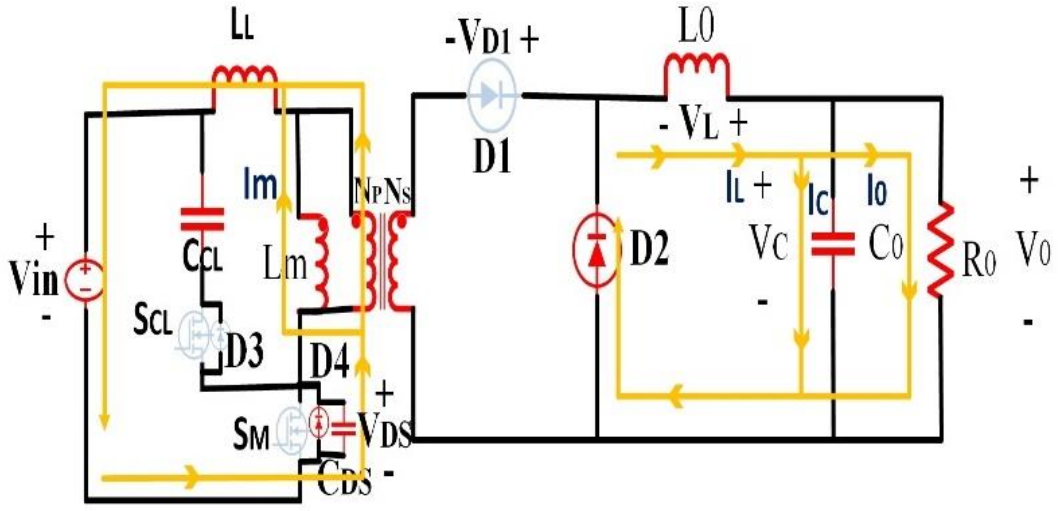

Fig. 4.5 Magnetising current and drain-source capacitance is discharging to the supply.

4.3 PROCEDURE FOR DESIGNING ACTIVE CLAMP FORWARD CONVERTER

D_{max} is the maximum duty cycle, occurs when voltage is maximum. D_{min} is the minimum-duty cycle, occurs when voltage is minimum. Therefor the value of filter inductor is given by,

$$L_0 = \frac{V_0(1-D_{min})}{\Delta I_{L0} I_0 F_S} \quad (4.8)$$

Where, ΔI_L is the ripple in the inductor current, and it is expected to be 5% of the present load I_0.

$$Q = \frac{0.5\Delta I_{LO}}{2F_S} \quad (4.9)$$

$$C_{0min} = \frac{Q}{\Delta V_0} \quad (4.10)$$

Where, ΔV_0 is ripple in output voltage(V_0), which is expected to 1% of output voltage.

$$R_0 = \frac{V_0^2}{P_0} \quad (4.11)$$

$$C_{CL} \geq \frac{10(1-D_{min})^2}{L_{mag}(2\pi F_s)^2} \quad (4.12)$$

Here, F_S is the switching frequency, L_0_is output inductance, Q is charge, C_{0min}_is the minimum value of output capacitance, R_0_is the output resistance, L_{mag} is the magnetising inductance of transformer and C_{CL} is clamp capacitance.

4.4 SIMULATION RESULTS

4.4.1 SIMULATION RESULTS AND DISCUSSION

In this study, active clamp forward converter_(ACFC) for transfer of about 488.6W power at a supply voltage of Vin = 100V and output voltage V0 = 14V is designed & simulated in MATLAB/Simulink. The design specifications of ACFC is illustrated in Table6.1 and Table6.2. A MATLAB model of the proposed scheme is developed for simulation.

4.4.2 PARAMETERS & COMPONENT VALUES

Table 4.1 Design specifications of Active clamp forward converter

Parameters	Value
Supply voltage (Vin)	100V
Supply Current (Iin)	10.67A
Switching frequency (Fs)	250kHz
Output voltage (V0)	14V

Output Current (I0)	34.95A
Output power (P0)	488.6W

Table 4.2 Component values and setting of controllers in Active clamp forward converter

Components	Values
CCL	133.7nF
Kp	0.0001
Ki	5
C0	622.4μF
L0	14μH
R0	0.4 Ω

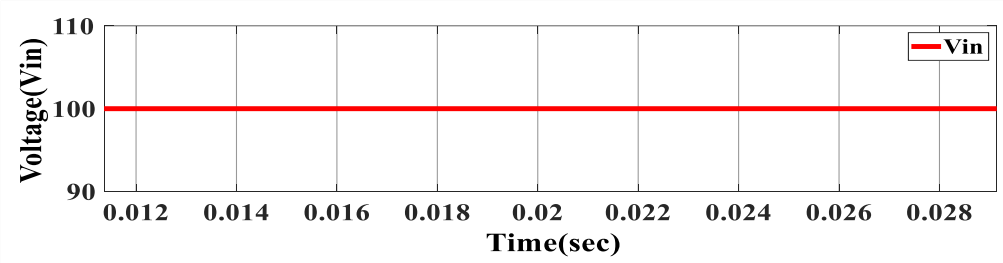

Fig. 4.6: Supply-Voltage

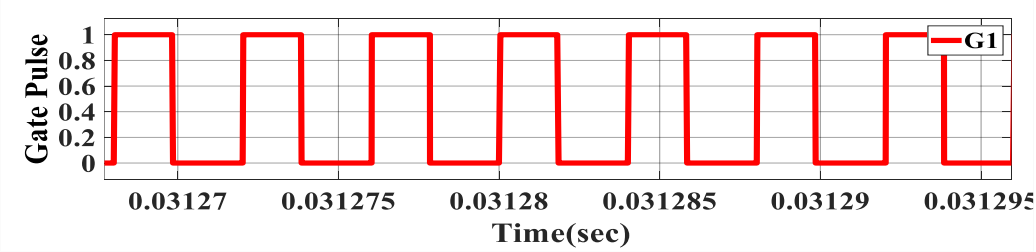

Fig. 4.7: Switching Pulse to main switch

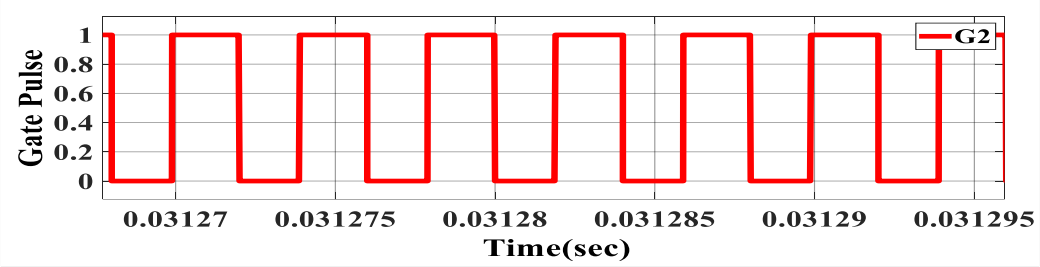

Fig. 4.8: Switching Pulse to clamp switch

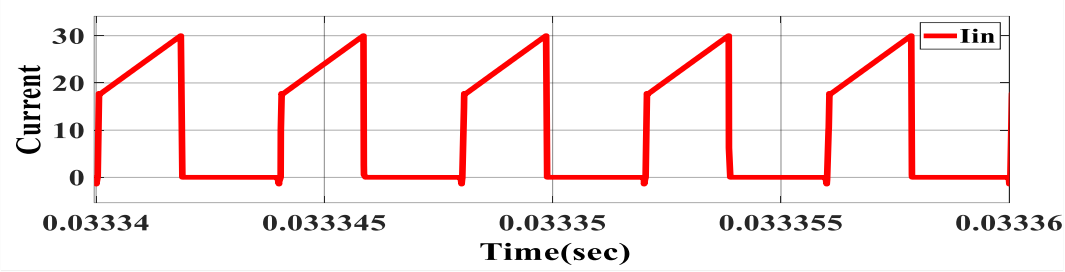

Fig. 4.9: Input Current

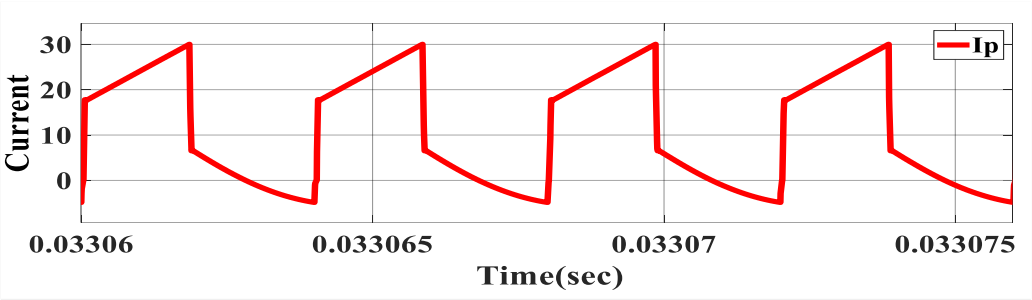

Fig. 4.10: Transformer Primary Side Current

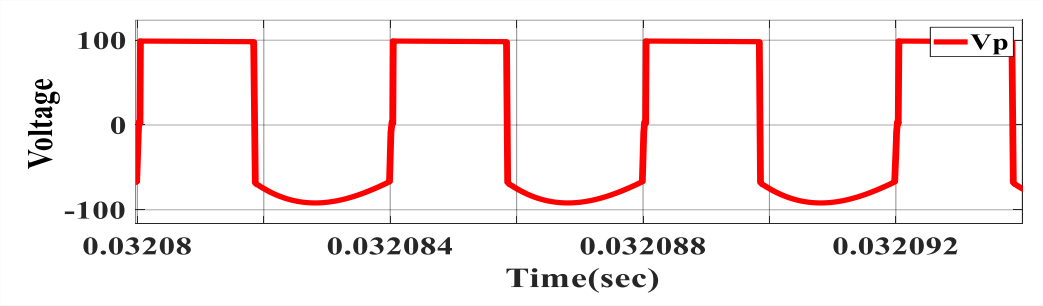

Fig. 4.11: Transformer primary Side Voltage

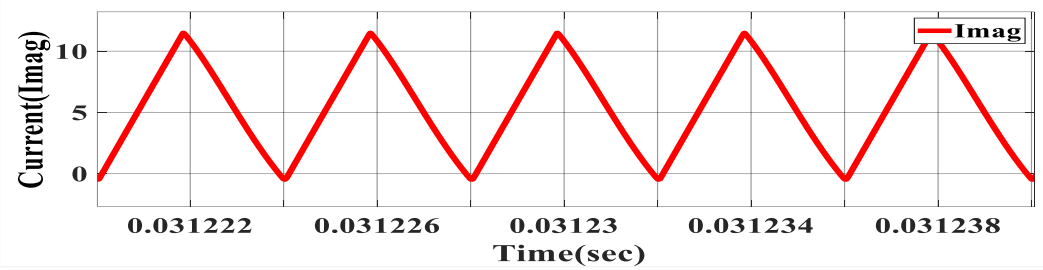

Fig. 4.12: Magnetising Current

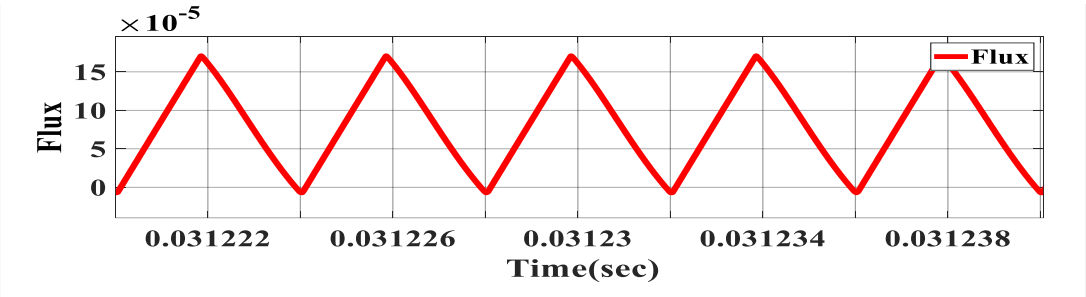

Fig. 4.13: Flux through Transformer

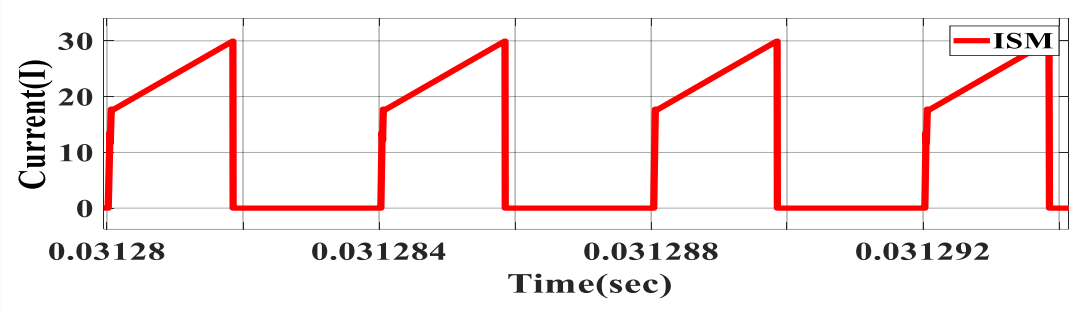

Fig. 4.14: Current through main switch_(SM) when ON

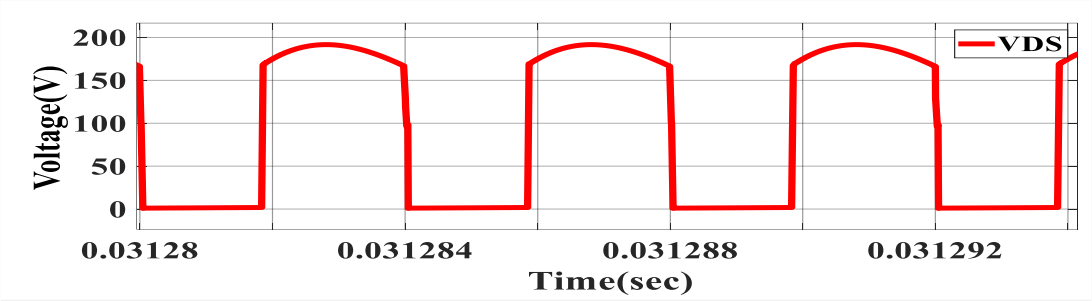

Fig. 4.15: Voltage across main switch_(SM) when OFF

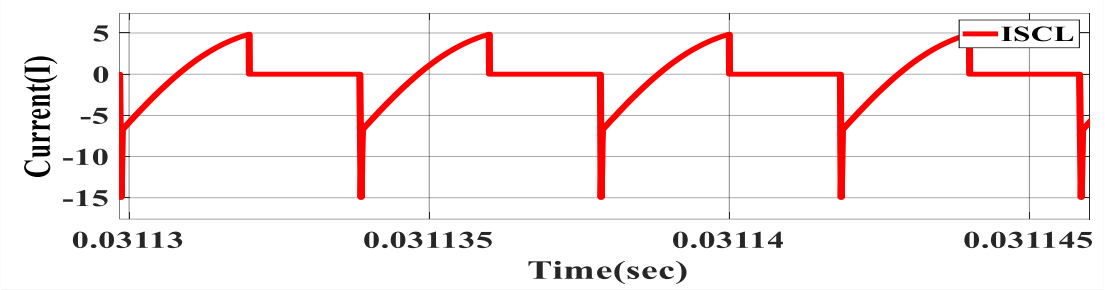

Fig. 4.16: Current through clamp switch_(SM) when ON

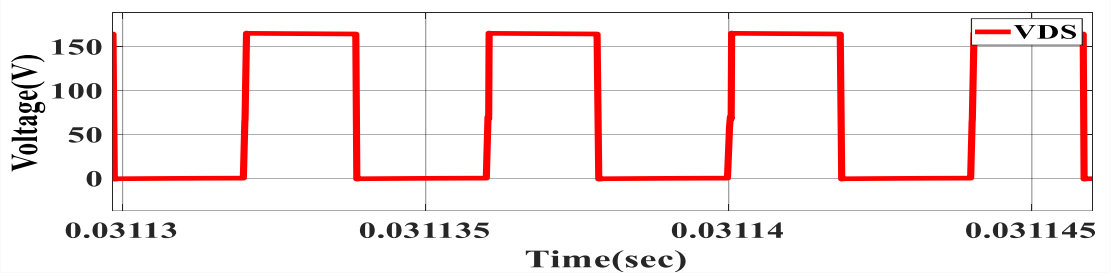

Fig. 4.17: Voltage across clamp switch_(SM) when OFF

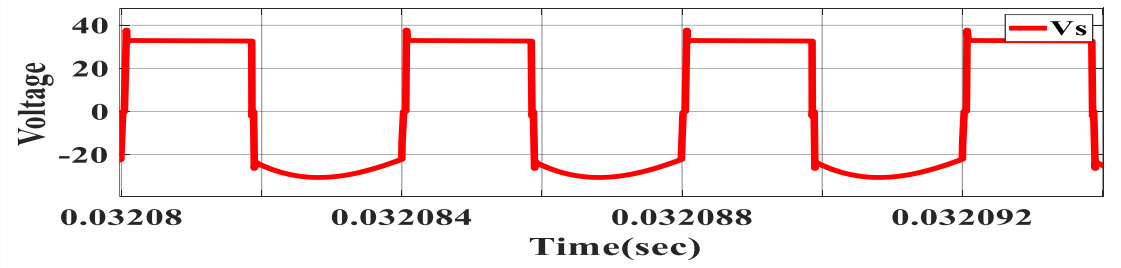

Fig. 4.18: Transformer Secondary Voltage

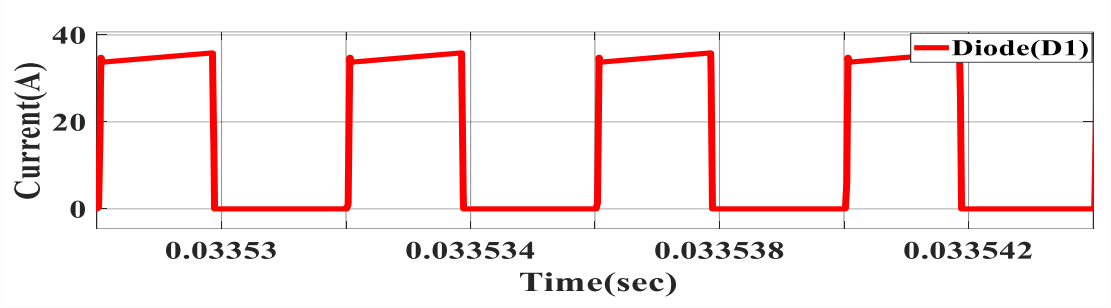

Fig. 4.19: Current through diode_(D1)

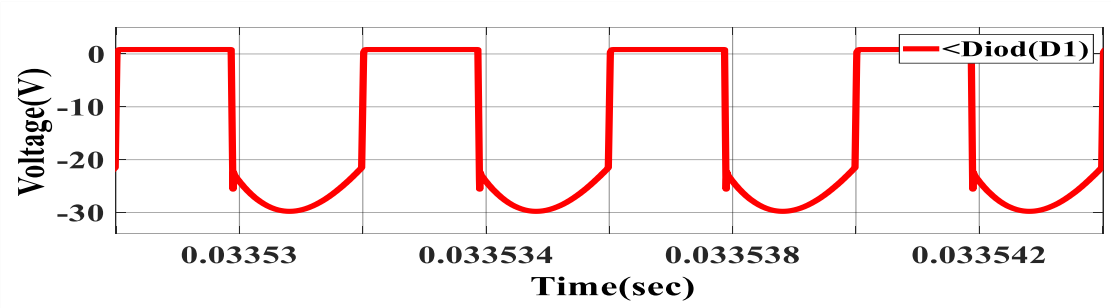

Fig.4.20: Voltage through diode_(D1)

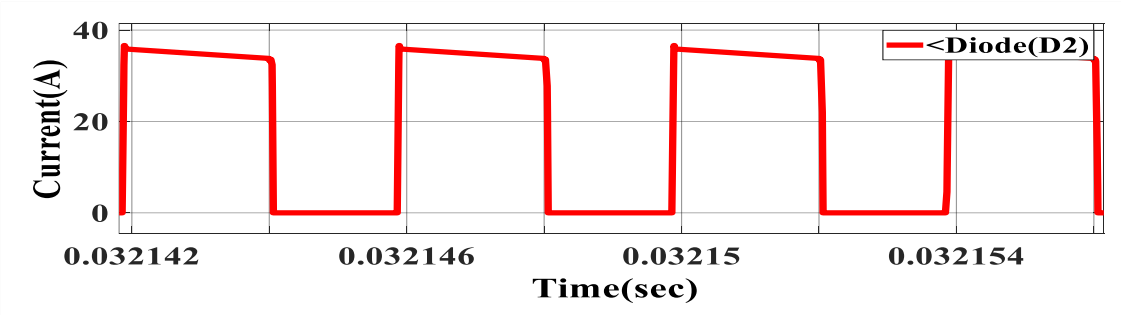

Fig. 4.21: Current through diode_(D2)

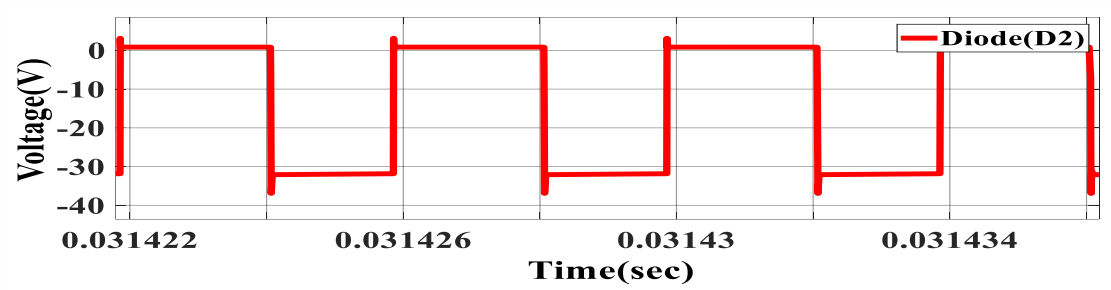

Fig.4.22: Voltage through diode(D2)

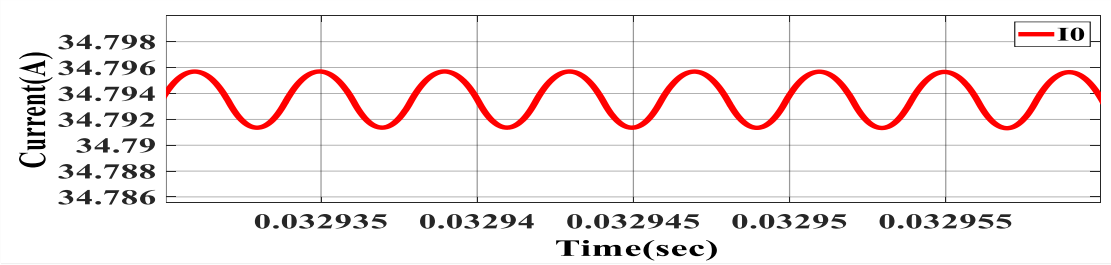

Fig. 4.23: Output Current

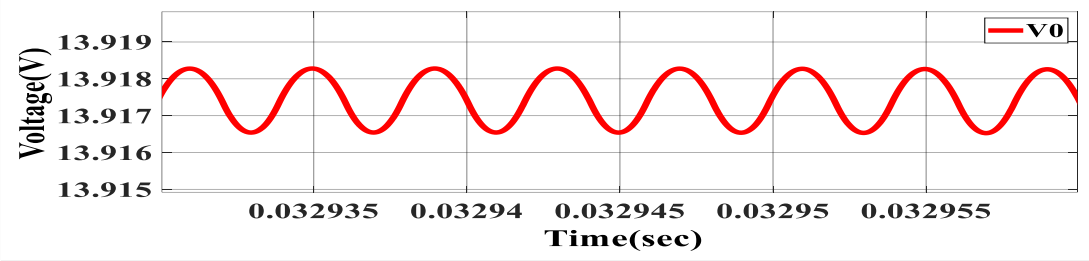

Fig. 4.24: Output Voltage

An active clamp forward converter's circuit_(ACFC) modelling is carried out in MATLAB/Simulink. **Fig.4.1** show the model of the converter. The input power-supply for ACFC prototype is a 100V, 10.67A dc-power source as illustrated in **Fig.4.6-Fig.4.9**. **Fig.4.7-Fig.4.8** show the gate pulse applied across main switch and the clamp switch for an supply voltage of 100V. Applied gate pulse width changes with increase in the input voltage and also a dead band of 1ns is applied for ON and OFF time of the switches. **Fig.4.10 to Fig.4.11** illustrate that, when the switch_(S_M) i.e., main switch is ON, switch_(S_{CL}) i.e., clamp switch_(C_{CL}) is OFF, the voltage across the S_{CL} and winding_(N_P) is the input voltage_(V_{in}), the current increases linearly through transformer primary winding. The current through the winding_(N_P) and the main switch_(S_M) is same and will be the summation of magnetising current_(I_m) and the secondary current referred to primary side_(I'_S). While when the switch_(S_M) is OFF and the switch_(S_{CL}) is ON magnetising current_(I_m) start discharging through the clamp capacitor_(C_{CL}) as shown in **Fig.4.16** and transformer reset take place. Reset of transformer is necessary during one complete switching period because the magnetising flux in the core of a transformer circuit must revert at its initial state after each switching cycle_(f_s) for periodic voltage and current operation. other-wise increase in magnetising current_(I_m) gradually in each switching period leads to saturation of transformer. The stored potential energy in the clamp capacitor_(C_{CL}) because of the magnetising current_(I_m) will be released and because of this energy magnetising current begun to build in reverse direction as illustrated in **Fig.4.10**. **Fig.4.12-Fig.4.13** show that magnetising current_(I_m) through the transformer. It is observed from **Fig.4.12-Fig.4.13** that transformer flux will be reset at the end of each switching period. **Fig.4.18 to Fig.4.22** are the current and voltage across secondary side diode i.e D1 and D2. **Fig.4.23 to Fig.4.24**. The DC output current and voltage, can be used to power up various parts of electric vehicles.

4.5 CONCLUSION

The active clamp forward converter's comprehensive circuit and mathematical analysis are presented in this chapter. To accomplish ZVS functioning of the main-switch_(S_M), the auxiliary clamp circuit is employed for reset the stored energy inside the leakage inductance_(L_L). Through use of synchronous FETs, the reduction of switching-losses in the main FET owing to ZVS, as well as the non-dissipative reset of a transformer recycling leaky inductive energy back to the input are all possible with the active clamp added to the forward converter. Another advantage is that soft switching reduces EMI, making this topology perfect for low-noise applications.

To manage output voltage(V_0), a PI-controller is being used which also decrease damping in the system, and the converter functioning in closed loop is proven for a fixed output voltage of 14V. The proportional-gain_(K_p) is set at 0.0001 for this setup, while integral-gain_(K_i) is set to 5. To accomplish ZVS functioning of the main switch, to reset the stored energy held in magnetising and leaking inductances, the clamp circuit is used. An ACFC is being implemented using input voltage supply of 80 to 120 volts and a supply current of 10.62 amps with an output voltage(V_0) of 14 volts, output current(I_0) of 34.95 amps, and an output power of 488.6W.

CHAPTER-5

MAIN CONCLUSIONS AND FUTURE SCOPE OF WORK

5.1 MAIN CONCLUSIONS

The research work presented in this dissertation has focused on design and implementation of WPT and Active Clamp Forward Converter_(ACFC) for EV applications. WPT is used to charge the Electric Vehicles Battery while Active Clamp Forward Converter_(ACFC) is used as a auxiliary power supply i.e. it is used to supply power to different parts of electric vehicles like light, horn and indicator etc by harnessing power from battery of electric vehicles. Wireless Power Transfer will be helpful in minimizing the battery size and weight of electric vehicles and also helpful in minimizing the overall cost of Electric Vehicles.

5.2 RECOMMENDATIONS FOR FUTURE WORK

The following plan of actions are suggested for future work on these converter topology :

1. Analysis of power inverter to reduce voltage spikes across the switches through modification in circuit topology.
2. Coils design and inductance analysis & simulation for improved bandwidth and mutual inductance.
3. A new topology of power amplifier may be adopted to boost efficiency at a lower cost.
4. With use of GaN devices, higher-frequency of operation could be demonstrated, which can assist in minimising circuit size.
5. By lowering the number of elements in the rectifier circuit, the overall efficiency of the converter could be enhanced.
6. To explore distance tracking analysis in the converter circuits.
7. Analysis on battery charging in closed loop mode.

Finally, this study mainly emphasizes that the growing need of electrical vehicle technology requires multidisciplinary collaboration between engineering science and

power utilities to tackle real-world challenges. WPT is a highly intriguing issue for real-world applications these days.

Here in this dissertation work Active Clamp Forward Converter_(ACFC) with voltage control mode is presented and analyzed. For more accurately tracking the output it may be extended to current control mode.

There are two type of current control mode: -

(i). Average Current Control Mode

(ii).Peak Current Control Mode

In average current control mode, the average inductor current is tracked and this average current control mode will give satisfactory performance when supply current and average inductor current are same i.e., it will track output more accurately in case of boost converter. While peak current mode control give performs well when output current and average inductor current are same i.e., it will track output more accurately in case of buck converter. Therefor in Active Clamp Forward Converter_(ACFC) peak current mode control for tracking output is explored.

APPENDIX-A

Simulation Parameters of Wireless Power Transfer:

Input Parameter 100W, 25V, 100KHz
Output Parameter 85.47W, 23.18V

L_f=485.43µH, C_1=41.74Nf, C_r=25.69nf, L_r=112.45µH, R_L=7.06Ω, C_P=21.7nf, L_P=116.68µH, C_S=31.416nf, L_S=80.62µH, M=9.68µH, K_C=0.1, C=6.57µ, L=42.98µH, R_0=6.25Ω

APPENDIX-B

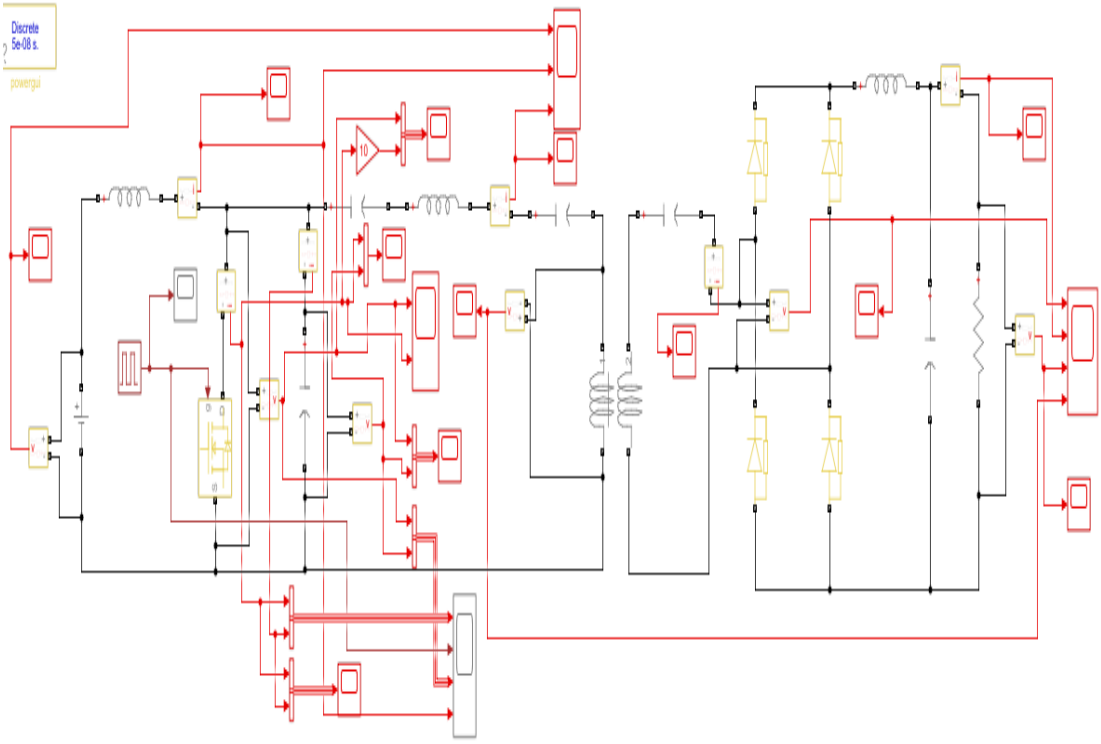

APPENDIX-C

Simulation Parameters of Active Clamp Forward Converter

Input Parameter 100V, 250KHz, 10.67A

Output Parameter 488.6W, 14V, 34.95A

C_{CL}=133.7nF, K_p=0.001, K_i=5, C_0=622.4µF, L_0=14µH, R_0=0.4Ω

APPENDIX-D

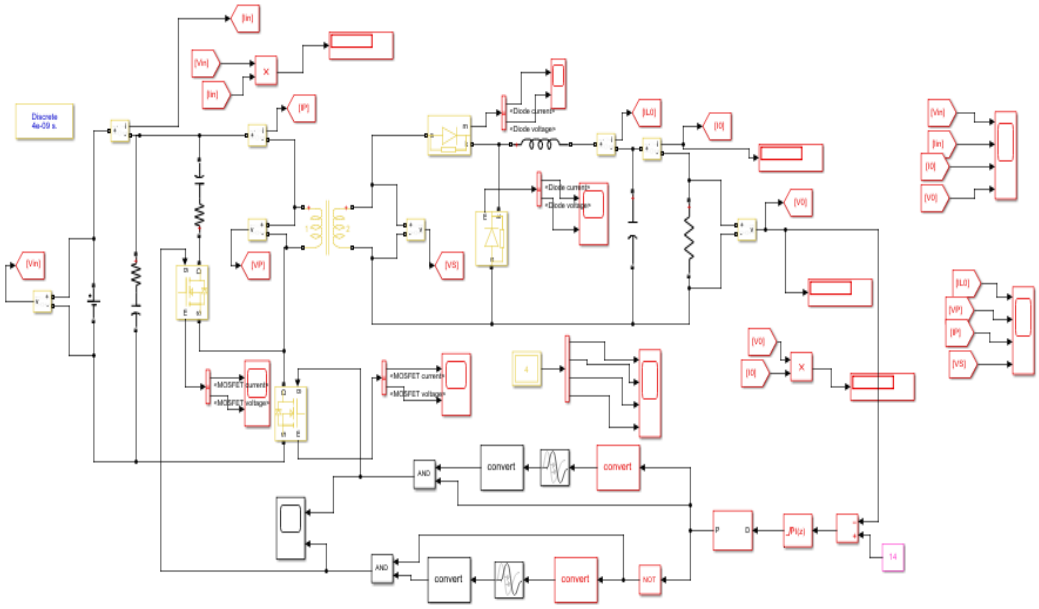

REFERENCES

[1] Li, Siqi, and Chunting Chris Mi. "Wireless power transfer for electric vehicle applications." IEEE journal of emerging and selected topics in power electronics 3, no. 1 (2014): 4-17.

[2] Zhang, Zhen, Hongliang Pang, Apostolos Georgiadis, and Carlo Cecati. "Wireless power transfer—An overview." IEEE Transactions on Industrial Electronics 66, no. 2 (2018): 1044-1058.

[3] Kurs, Andre, Aristeidis Karalis, Robert Moffatt, John D. Joannopoulos, Peter Fisher, and Marin Soljacic. "Wireless power transfer via strongly coupled magnetic resonances." science 317, no. 5834 (2007): 83-86.

[4] Darvish, P., Mekhilef, S., & Illias, H. A. B. (2020). A novel S–S–LCLCC compensation for three-coil WPT to improve misalignment and energy efficiency stiffness of wireless charging system. IEEE Transactions on Power Electronics, 36(2), 1341-1355.

[5] Kalwar, K. A., Aamir, M., & Mekhilef, S. (2018). A design method for developing a high misalignment tolerant wireless charging system for electric vehicles. Measurement, 118, 237-245.

[6] Hossain, A., Darvish, P., Saad, M., SOON, T. K., & Chong, W. T. (2021). A New Coil Structure of Dual Transmitters and Dual Receivers with Integrated Decoupling Coils for Increasing Power Transfer & Misalignment Tolerance of Wireless EV Charging System. IEEE Transactions on Industrial Electronics.

[7] M.Kazimierczuk and D.Czarkowski, “Resonant power converters,” John Wiley &Sons, 2nd Edition, 2011

[8] R.J.Cardesin, J.Garcia, J.Dalla-Costa and J.M.Alonso, “Electronic ballast for metal halide lamps based on a class E resonant inverter operating at 1MHz,” IEEE 20th Annual Applied Power Electronics Conference and Exposition, Mar.2005, pp.600-604

[9] T. Suetsugu and M. Kazimierczuk, “Analysis of transient behavior of Class E amplifier due to load variations”, IEEE Conference on Power Electronic and Drive Systems PEDS, February 2011, Singapore.

[10] A. Kurs, A. Karalis, R. Moffatt, J. D Joannopoulos, P. Fisher, M. Soljacic, " Wireless power transfer via strong coupled magnetic resonance", Science Express, vol. 317, 2007.

[11] A. P. Sample, D. J. Yeager, P. S. Powledge, A. V. Mamishev, and J.R. Smith, "Design of an RFID-based battery-free programmable sensing platform," IEEE Transactions on Instrumentation and Measurement, vol. 57, no. 11, pp. 2608–2615, 2008.

[12] A. Karalis, J. D. Joannopoulos, and M. Soljaˇci´c, "Efficient wireless non radiative mid-range energy transfer," Annals of Physics, vol. 323, no. 1, pp. 34–48, 2008.

[13] M. Shoyama, G. Li and T. N inomiya, "Application of common- source active-clamp circuit to various DC-DC converter topologies", IEEE-PESC Conference, vo1. 3, pp. 1 32 I -1326, 2003.

[14] R. E. Hamam, A. Karalis, J. D. Joannopoulos, andM. Soljaˇci´c, "Efficient weakly-radiative wireless energy transfer: an EIT-like approach," Annals of Physics, vol. 324, no. 8,pp. 1783–1795, 2009.

[15] Z. N. Low, R. A. Chinga, R. Tseng, and J. Lin, "Design and test of a high-power high-efficiency loosely coupled planar wireless power transfer system," IEEE Transactions on Industrial Electronics, vol. 56, no. 5, pp. 1801–1812, 2009.

[16] L. Chen, S. Liu, Y. C. Zhou, and T. J. Cui, "An optimizable circuit structure for high-efficiency wireless power transfer," IEEE Transactions on Industrial Electronics, vol. 60,no. 1, pp. 339–349,2013.

[17] M. Kiani and M. Ghovanloo, "The circuit theory behind coupled-mode magnetic resonance-basedwireless power transmission,"IEEE Transactions on Circuits and Systems. I. Regular Papers, vol. 59, no. 9, pp. 2065–2074, 2012.

[18] J. de Boeij, E. Lomonova, J. L. Duarte, and A. J. A. Vandenput,"Contactless power supply for moving sensors and actuators in high-precision mechatronic systems with long-stroke power transfer capability in x-y plane," Sensors and Actuators A: Physical, vol. 148, no. 1, pp. 319–328, 2008.

[19]P. Li and R. Bashirullah, “A wireless power interface for rechargeable battery operated medical implants,” IEEE Transactions on Circuits and Systems II: Express Briefs, vol. 54, no. 10,pp. 912–916, 2007.

[20]P. Si, A. P. Hu, S.Malpas, and D. Budgett, “A frequency control method for regulating wireless power to implantable devices,” IEEE Transactions on Biomedical Circuits and Systems, vol. 2, no.1, pp. 22–29, 2008.

[21]J. L. Villa, J. Sall´an, A. Llombart, and J. F. Sanz, “Design of a high frequency inductively coupled power transfer system for electric vehicle battery charge,” Applied Energy, vol. 86, no. 3,pp. 355–363, 2009.

[22]S. Jones, G. Bucea, A. McAlpine et al., “Condition monitoring system for TransGrid 330kV power cable,” in Proceedings of the International Conference on Power SystemTechnology (POWERCON’04), pp. 1282–1287, Singapore,November 2004.

[23]E. Gulski, P. Cichecki, J. J. Smit, P. P. Seitz, B. Quak, and F.de Vries, “On-site condition monitoring of HV power cable up to 150kV,” in Proceedings of the International Conference on Condition Monitoring and Diagnosis (CMD ’08), pp. 1199–1202,April 2008.

[24]N. Inagaki, “Theory of image impendence matching for inductively coupled power transfer systems,” IEEE Transactions on MicrowaveTheory and Techniques, vol. 62, pp. 901–908, 2014.

[25]R. Roberts, “Conjugate-image impendences,” Proceeding of the IRE, vol. 34, no. 4, pp. 198–204, 1946.

[26]M. Kiani, U.-M. Jow, and M. Ghovanloo, “Design and optimization of a 3-coil inductive link for efficient wireless power transmission,” IEEE Transactions on Biomedical Circuits and Systems, vol. 5, no. 6, pp. 579–591, 2011.

[27]A. P. Sample, D. A. Meyer, and J. R. Smith, “Analysis, experimental results, and range adaptation of magnetically coupled resonators for wireless power transfer,” IEEE Transactions on Industrial Electronics, vol. 58, no. 2, pp. 544–554, 2011.

[28]T. C. Beh, M. Kato, T. Imura, S. Oh, and Y. Hori, “Automated impedance matching system for robust wireless power transfer via magnetic resonance

coupling," IEEE Transactions on Industrial Electronics, vol. 60, no. 9, pp. 3689–3698, 2013.

[29]R. Watson, F. C. Lee, and G. C. Hua, "Utilization of an active- clamp circuit to achieve soft switching in flyback converters", IEEE Transactions on Power Electronic, vol. 11, no. 1, pp. I 62- 1 69, 1996.

[30]Q. M. Li and F. C. Lee, "Design consideration of the active- clamp forward converter with current mode control during large- signal transient", IEEE Transactions on Power Electronics, vo1. 18, no. 4, pp. 958-965, 2003.

[31]R. Torrico-Bascop and N. Barbi, "A double ZVS-PWM active- clamping forward converter: analysis, design, and experimentation", IEEE Transactions on Power Electronics, vol. 1 6, no. 6, pp. 745-751, 2001.

[32]B. S. Lim, K. W. Lee, S. H. Woo and J. K. Hee, "A new self- driven active clamp forward converter using the auxiliary winding of transformer", IEEE INTELEC Conference, pp. l 64- 168, 2002.

[33]D. J itaru and S. Birca-Galateanu, "Small-signal characterization of the forward-flyback converters with active clamp", IEEE-APEC Conference, vol. 2, pp. 626-632, 1998.

[34]C. T. Choi, C. K. Li and S. K. Kok, "Modeling of an active clamp discontinuous conduction mode flyback converter under variation of operating conditions", IEEE-PEDS Conference. vo1. 2, pp. 730-733, 1999.

[35]UCC289/1/2/3/4 Current-Mode Active Clamp PWM Controller, Datasheet (SLUS542)

[36]UCC2897 Current-Mode Active Clamp PWM Controller, Datasheet (SLUS591A)

[37]UCC3580/-1/-2/-3/-4 Single Ended Active Clamp Reset PWM, Datasheet, (SLUS292A)

[38]Steve Mappus, UCC2891EVM, 48-V to 1.3-V, 30-A Forward Converter with Active Clamp Reset,User's Guide to Accommodate UCC2891EVM, (SLUU178)

[39] Steve Mappus, Reference Design PR265A 48V to 3.3V Forward Converter with Active Clamp Reset Using the UCC2897 Active Clamp Current Mode PWM Controller, (SLUU192)

[40] B R Lin, F.-Y. Hsieh, D. Wang, and K. Huang, Analysis, design and implementation of active clamp zero voltage switching converter with output ripple current cancellation, IEE Proc.-Electr. Power Appl., 153, 2006, pp.653–656.

[41] Lin, B.-R.; Shih, H.-Y., IET Power Electronics, Implementation of a parallel zero-voltage switching forward converter with less power switches, vol.4, no.2, 2011 pp.248-256.

[42] Hongfei Wu; Peng Xu; Wei Liu; Yan Xing, Series-Input Interleaved Forward Converter with a Shared Switching Leg for Wide Input Voltage Range Applications, IEEE Transactions on Industrial Electronics, vol.60, no.11, 2013, pp.5029-5039.

[43] Praveen Jain,"Soft and resonant switching power electronics for a small urban electric vehicle", 2012 International Conference on Renewable Energy Research and Applications (ICRERA), pp.1 – 43, 2012.

[44] Kouhei Akamatsu; Tomokazu Mishima; Mutsuo Nakaoka, "A secondary-side phase-shifted zero voltage and zero current fullrangesoft-switching PWM DC-DC converter for EV battery chargers", 2012 International Conference on Renewable Energy Research and Applications (ICRERA), pp.1 – 6, 2012.

[45] Daisuke Tsukiyama; Yasuhiko Fukuda; Shuji Miyake; Saad Mekhilef; Soon-Kurl Kwon; Mutsuo Nakaoka, "A novel type highefficiency high-frequency-linked full-bridge DC-DC converter operating under secondary-side series resonant principle for high-power PV generation", 2012 International Conference on Renewable Energy Research and Applications (ICRERA), pp.1 – 6, 2012.

[46] Bhanu Prashant Baddipadiga; Mehdi Ferdowsi,"Dual loop control for eliminating DC-bias in a DCDC dual active bridge converter", 2014 International Conference on Renewable Energy Research and Application (ICRERA), pp. 490-495, 2014.

[47]Muhammet Bibero÷lu; Taha Nurettin Gücin; Bekir Fincan, “Analyzing the influences of high frequency transformers utilized in parallel resonant converters”, 2016 International Conference on Renewable Energy Research and Application (ICRERA), pp. 983-988, 2016.

LIST OF PUBLICATIONS

1. Design and Implementation of Wireless Power Transfer Using Class-E Resonant Inverter and Magnetic Resonance Coupling. Accepted in IEEE IAS (GlobConET) 2022 Global Conference on Emerging Technologies to be held on May 20-22, 2022
   Organised by:- GlobCoET
2. Design and Implementation of Active Clamp Forward Converter for Electric Vehicle Applications. Accepted in 2nd International Conference on Signals, Machines, and Automation *(SIGMA)-2022*
   Organised by:- Netaji Subhas University of Technology (NSUT)